1-1-1984

A study of nonlinear transconductance in synchronous oscillators.

Theodore D. Flamouropoulos

A STUDY OF NONLINEAR TRANSCONDUCTANCE IN SYNCHRONOUS OSCILLATORS

BY

THEODORE D. FLAMOUROPOULOS

A Thesis
Presented to the Graduate Committee
of Lehigh University
in Candidacy for the Degree of
Master of Science
in the Department of
Computer Science and Electrical Engineering

Lehigh University
December, 1984

A STUDY OF NONLINEAR TRANSCONDUCTANCE IN SYNCHRONOUS OSCILLATORS

BY

THEODORE D. FLAMOUROPOULOS

A Thesis
Presented to the Graduate Committee
of Lehigh University
in Candidacy for the Degree of
Master of Science
in the Department of
Computer Science and Electrical Engineering

Lehigh University
December, 1984

This thesis is accepted and approved in partial fulfillment of the requirements for the degree of Master of Science.

December 17, 1984
Date

Professor in Charge

Chairman of the Department

ACKNOWLEDGEMENTS

The author is grateful to Dr. Marvin H. White for invaluable insights, assistance and encouragement provided throughout this study. Special thanks are due to Dr. Vasil Uzunoglu for technical advice and for creating the opportunity to study the Synchronous Oscillator. Great thanks are due to my wife Elise for tireless help and moral support in the preparation of this thesis and to my mother Domna for investing in my future to make this work possible.

TABLE OF CONTENTS

List of Figures

ABSTRACT

The goal of this thesis is the identification of the major obstacles responsible for the slow progress in modeling synchronization in oscillators. A brief historical review reveals that a major difficulty with most synchronization models is the lack of analytical expressions for the nonlinear transconductance associated with the transistor within the oscillator. The circuit used for the investigation into the nature of nonlinear transconductance is the Synchronous Oscillator developed by Dr. Vasil Uzunoglu of Fairchild Industries. Experimental measurements via high bandwidth oscilloscope (Tektronix 7854) and network analyser (HP 3577A) uncovered certain clues that form the basis of a mathematical analysis. The analysis leads to an expression for the transconductance. The expression is finally simplified so as to become useful for analytical investigations of synchronization in the Synchronous Oscillator.

1. INTRODUCTION: An Historical Perspective

Synchronization is a concept of rarely appreciated dimensions. It is encountered in the natural world at every conceptual level from the microscopic to the macroscopic. Examples of synchronization behavior abound in animate and inanimate systems. Synchronization is the ability of an oscillating system to mimic another oscillating system. The most famous observation of this phenomenon was recorded by Huygens. He noticed that two pendulum clocks hung on the same supporting plank behaved in a peculiar manner. Despite a difference in the natural frequencies of the two clocks, they tended to oscillate at a common frequency with only a phase difference. Identical oscillation with a constant phase difference seems to be the common thread running through most synchronization phenomena.

Huygens' supporting plank was instrumental in the creation of conditions favorable for synchronization. In fact, it was via the supporting plank that the clocks were able to influence each other. It is implicit in any theory of synchronization that there must be a link through which one system may influence another. Living systems such as courting birds may require visual and/or audio links to accomplish synchronization. Oscillating heart cells require physical proximity to attain synchronization with other heart cells. Electrical systems require electromagnetic signals as the link needed for synchronization.

In electrical engineering and specifically in communications, synchronization is a very important and useful phenomenon. The phenomenon is indispensible for synchronous communication between two systems. For example, synchronization is used in a carrier recovery subsystem that makes demodulation of a signal possible. Synchronization is also used in the extraction of timing information from a signal.

The structure within a communication system responsible for synchronization is known as a synchronization network. This network tracks the carrier component of an external signal entering the communication system. There are two distinct approaches used in the design of synchronization networks. One scheme makes use of the "phaselock" principle. The other scheme relies on the use of nonlinear oscillators.

2. SYNCHRONIZATION NETWORKS

2.1 The Phase Locked Loop

A Phase Locked Loop (PLL) embodies the "phaselock" principle. The PLL is composed of a phase detector, a low pass filter and a voltage controlled oscillator (VCO) as illustrated in figure 2-1. The phase detector compares two signals and produces an output equal to the sine of the phase difference between the two signals. The VCO is an oscillator whose frequency is controlled by the magnitude of a d.c. input.

In operation, the phase detector compares an external signal to the output of the VCO. The sine of the phase difference is filtered to remove higher harmonics and noise produced in the phase detector. The output of the filter is presented to the input of the VCO, where a change in oscillation frequency occurs. The oscillation frequency continues to change until the phase difference between the VCO and the external signal becomes minimal and constant. At this point steady state has been achieved and the VCO is tracking the external signal at a constant phase difference. The description is obviously oversimplified, but it serves to illustrate the conceptual underpinnings of the "phaselock" principle.

PLLs are widely used in the communications field. The widespread popularity of PLLs is mainly due to the overall

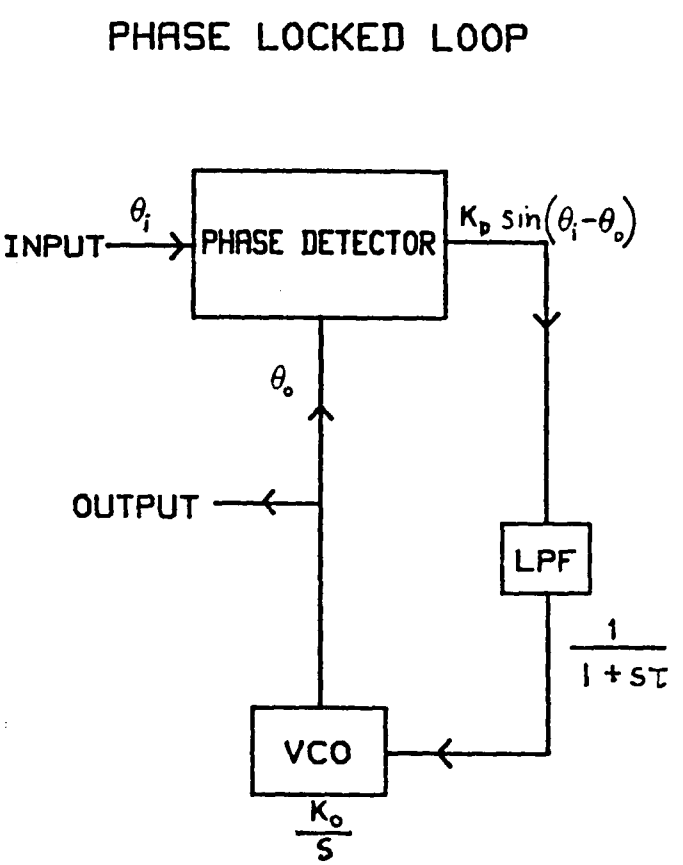

Figure 2-1: A simple system representation of a Phase Locked Loop.

simplicity of the scheme. Analysis of the PLL is very tractable because the "phaselock" principle is a linear concept. Problems arise when one considers nonlinearities due to most of the components of the PLL. For instance, the phase detector is a nonlinear element that outputs more than just the sine of the phase difference. The unwanted effects due to the nonlinearities are eliminated only at the expense of simplicity. Despite the increase in complexity PLLs remain the most modelable synchronization network.

The popularity of PLLs does nothing to reduce certain basic shortcomings that accompany such networks. PLLs are very susceptible to noise carried by the external signal. Approximately 5dB or more signal to noise ratio is needed for reliable operation. PLLs have relatively long acquisition times for many high frequency applications. Acquisition time is the interval required by the PLL to reach steady state after an external signal is introduced. The acquisition time is inversely related to the pull-in range of the PLL. Pull-in range is the bandwidth around the natural frequency for which the PLL will synchronize to the external signal. High frequency PLLs have high Q, small pull-in ranges and therefore large acquisition times.

Solutions to the problems just mentioned are not easy to implement. Such solutions can be complex, cumbersome and costly. One

exception is the work of Peter Runge [1]. Runge circumvented difficulties of acquisition in high Q PLLs by resorting to signal injection. The injection site was located at the VCO. The scheme resulted in increases of up to two orders of magnitude in the pull-in range of the PLL with corresponding decreases in the acquisition time.

2.2 The Nonlinear Oscillator

A second class of synchronization networks is composed of nonlinear oscillators. A nonlinear oscillator will exhibit behavior similar to a PLL when a signal is injected into the oscillator. The injected signal will cause the frequency of oscillation to shift until the frequency of the injected signal is identical to that of the oscillator. There will of course be a telltale phase difference between the oscillator and the injected signal. This synchronization in oscillators is also known as entrainment.

The mechanism responsible for entrainment in oscillators is assumed to be nonlinear. Analysis and modeling of this mechanism has traditionally been regarded as a difficult task. Difficulties with analysis have made oscillators very unattractive and unpopular as synchronization networks. However models for entrainment have been slowly and painstakingly developed over the past 50 years. My first goal is the evaluation of the applicability of such models to particular oscillator configurations.

3. NONLINEAR OSCILLATOR MODELS

3.1 The van der Pol Model

Considerable effort has been expanded in the analysis of nonlinear oscillators and the identification of the mechanism responsible for entrainment. Different approaches have been taken to simplify and/or avoid the nonlinearities. There are three main routes that have been investigated in search of a model for entrainment. Van der Pol was the first to attempt an analysis of a nonlinear oscillator [2]. His was a straightforward approach. He performed a circuit analysis and derived a second order nonlinear differential equation.

$$\ddot{x} + (\gamma x^2 - \alpha)\dot{x} + \omega_0^2 x = \omega_0^2 \, E \, \sin(\omega_1 t)$$

Van der Pol's equation is now widely accepted as an adequate representation of an oscillator. It is of course only an approximation. A solution to this equation was found by van der Pol. This solution is shown in figure 3-1. This figure forms the core of much subsequent work done on entrainment. The abscissa represents the frequency of the injected signal. The ordinate represents the magnitude of the oscillating output voltage. The different curves represent variation in the magnitude of the injected signal.

Looking at the figure it is immediately obvious that a stable solution to the equation is not always possible. Two types of

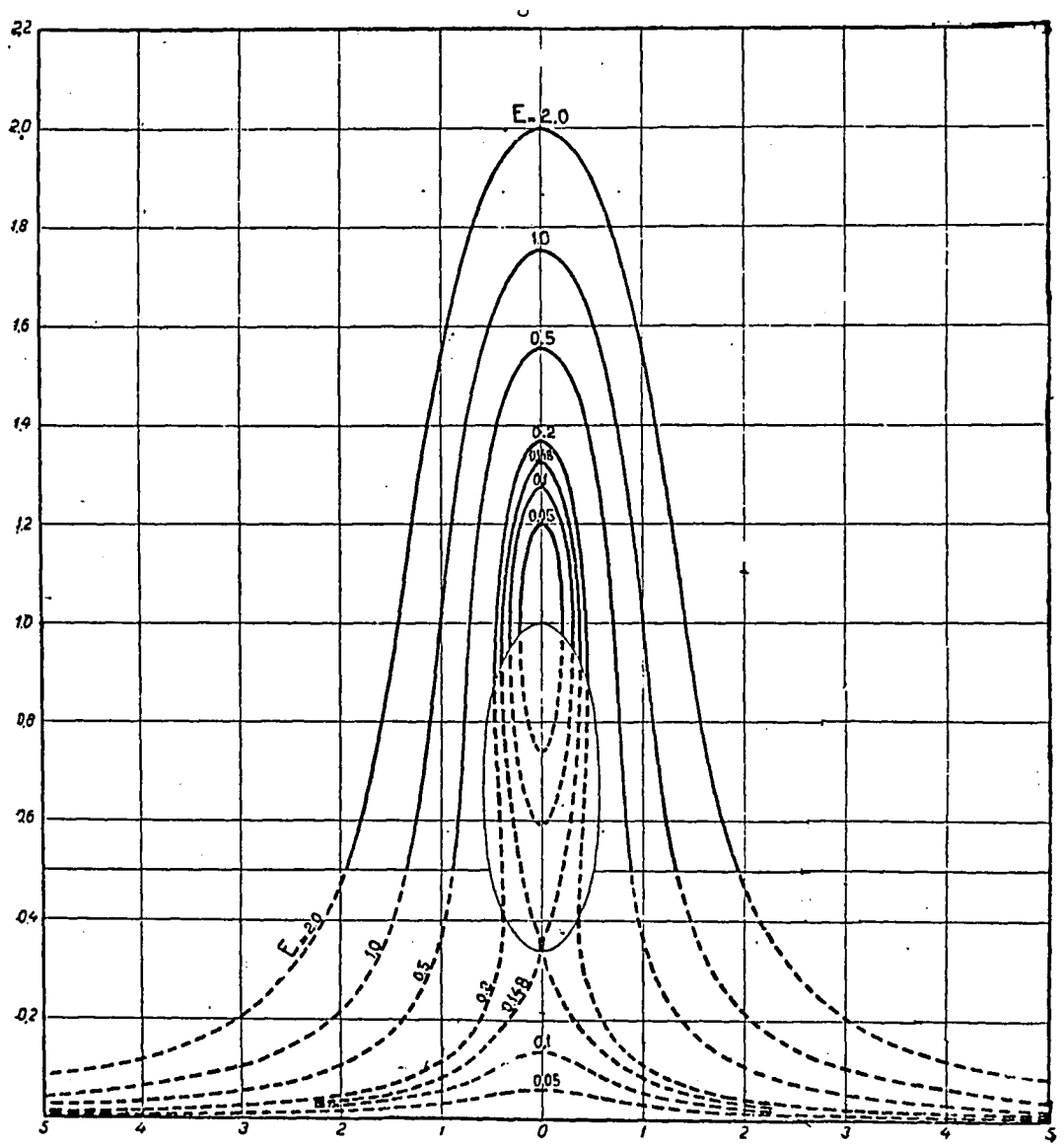

Figure 3-1: Solutions to van der Pol's equation for various input magnitudes. The ordinate represents magnitude of oscillation and the abscissa represents w/w_o. Dotted lines signify areas where solution does not exist.

phenomena were recognized within the stable solution of the van der Pol equation. These phenomena were called phaselocking (as in a PLL) and asynchronous quenching. Phaselock is a physical phenomenon where self-sustained oscillations synchronize to an injected signal. This behavior is similar to PLL operation. Phaselock is observed only for injected frequencies near the resonant frequency of the oscillator. Asynchronous quenching is a phenomenon where the injected signal destroys the self-sustained oscillations. The result is a passive resonator driven by the injected signal. This behavior is observed far away from the resonant frequency.

A good deal of controversy has followed these two terms through the years. The object of the controversy has been a disagreement over the origins of the two phenomena. Some researchers [3] have insisted that quenching and phaselock are products of a single mechanism. Others [4] have proposed that the two are distinctly different phenomena. An attempt to resolve the matter resulted in a long and convoluted exchange between researchers in the pages of an IEEE journal. The dispute was finally settled by E.M Dewan [5]. At the conclusion of a lengthy paper, Dewan stated that phaselock and asynchronous quenching are physically distinct mechanisms. He also went a step further and subdivided quenching into active and passive quenching.

The arguments over interpretation of physical phenomena

illustrate the inadequacies of the van der Pol solution. The solution cannot predict distinct and logically obvious mechanisms to satisfy the physical evidence. Dewan attempts in his article to explain these phenomena in terms of the van der Pol solution. He is however, encumbered by the severe approximations made in the van der Pol equation. His explanations rely heavily on mathematical concepts such as saddle points and poles that provide very little physical understanding. There is a growing need for a more accurate version of the van der Pol equation: a version that can better model the phenomenon of entrainment.

3.2 The Adler Model

A second study of synchronization was conducted by Robert Adler [6]. Adler chose a phenomenological path in his analysis of synchronization in oscillators. The Adler model is shown in figure 3-2. Adler developed a scheme that eliminated the nonlinearities associated with oscillators. He represented all elements outside the tuned circuit of his oscillator by a nonlinear negative resistance. Over a long period of time the negative resistance would adjust itself so as to become equal to the positive losses of the tuned circuit. The cancellation of losses would make the oscillator appear as a purely reactive tuned circuit.

Adler defined two constraining conditions that described the region in which his solutions were valid. He stated that any

ADLER MODEL

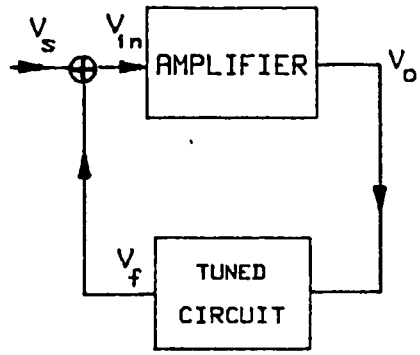

Figure 3-2: Adler's systems model for nonlinear oscillator.

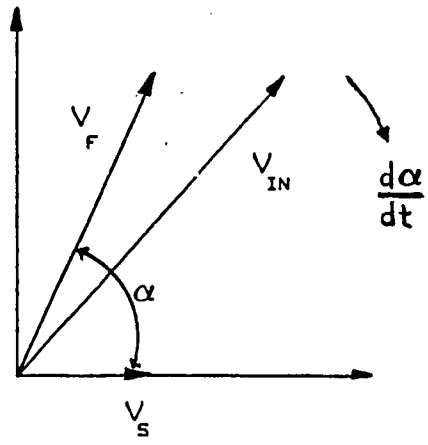

$$\frac{d\alpha}{dt} = -\frac{V_s \omega_0}{V_f 2Q} \sin(\alpha) + \Delta\omega_0$$

Figure 3-3: Summation of voltages at the input of the oscillator. Phasor notation indicates the rotation due to oscillations.

injected frequency must be close enough to the resonant frequency of the oscillator to assure the following:

1. That the phase difference between the external signal and the output of the tuned circuit is linear with respect to injected frequency.
2. That the amplitude of the oscillation does not change significantly with a change in frequency when synchronized.

The second condition depends greatly on the characteristic of the negative resistance. Adler also stated that only phase and amplitude information of the present would be used and no effects from conditions that existed previously could be allowed. Adler in effect linearized the problem to the fullest.

This framework set the stage for Adler's derivation of a differential equation for the oscillator phase as a function of time. To accomplish the derivation he used a vector representation of the summation of various voltages at the input of the oscillator as shown in Figure 3-3. The result of the analysis was the development of the differential equation that essentially models the acquisition process of the oscillator. An additional result was the derivation of an expression that predicted a bandwidth of synchronization. This was a band of frequencies around the resonance of the oscillator where phaselock was possible. This bandwidth was a function of the negative resistance, the resonant frequency and the magnitude of the output voltage.

Adler's approach was ingenious in avoiding most of the complications of nonlinear analysis. The price that he paid however was considerable. His model could not predict the steady state oscillation voltage of the oscillator. The model assumed that the nonlinearities are not important for small perturbations around the resonant frequency. The model is treated simply as a linear tank circuit around steady state. Nonlinearities manifest themselves within Adler's solutions in the form of an assumed oscillation voltage and an ill-defined transconductance of the active element. Finally it is impossible for the analysis to predict anything unless an oscillator is built and probed to ascertain the steady state oscillation voltage. The analysis is very useful however in the iterative design of oscillators.

3.3 The Kurokawa Model

A third approach in treating oscillators was suggested by Kurokawa [7]. The model used by Kurokawa is somewhat similar to that of Adler. A negative resistance is in series with a tuned circuit and an injected signal as shown in figure 3-4. The tuned circuit is assumed to have more than one resonance. The choice of models is the only explicit similarity between Kurokawa's and Adler's approaches. Whereas Adler tried to avoid nonlinearities, Kurokawa resolved to treat them.

Kurokawa brought the nonlinearities into his analysis in the

KUROKAWA MODEL

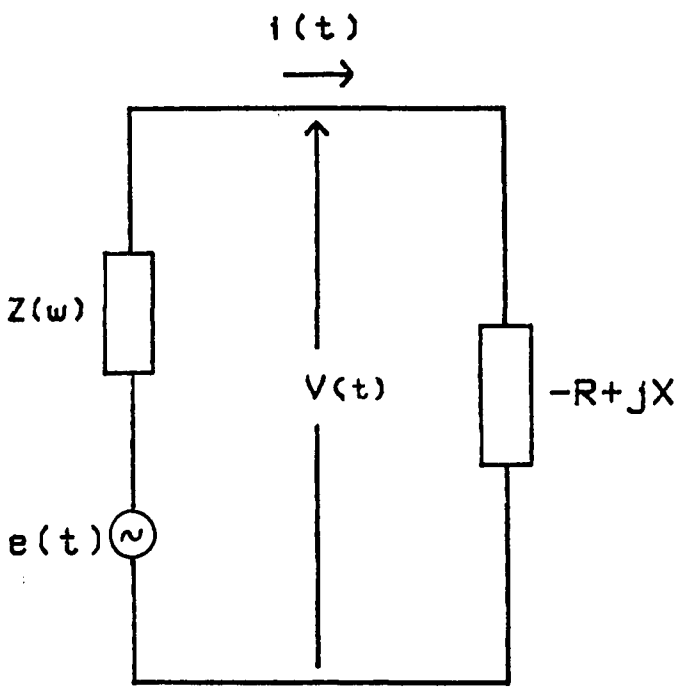

Figure 3-4: Kurokawa's model for an oscillator.

form of a current i(t) flowing through the active device that is responsible for the negative resistance. The current was assumed to be a sinusoid with a slow time-varying coefficient. In the analysis, this current was transformed to a plane similar to the complex plane. The transformation was accomplished through a clever observation of the properties of the derivative di(t)/dt. The transformation was assumed to have all the linear properties of a Laplace transformation.

To find the output voltage across the tuned circuit Kurokawa had to multiply the transform of the current i(t) to the impedance of the tuned circuit. The impedance was expressed in terms of the new transform plane. This clever use of an alternate transform is the key to Kurokawa's analysis. In the end Kurokawa was able to derive an expression for the bandwidth of synchronization just as Adler had done. Most importantly however, Kurokawa was able to predict the steady state oscillation voltage of the oscillator.

The three studies just discussed have become the theoretical foundations of synchronization in oscillators. The studies complement each other because they have widely different approaches. Each study had its own motivations, goals and tactics. Adler was interested in the bandwidth of synchronization. He was not interested in the detailed description of the nonlinear negative resistance that induces steady state nonlinear oscillations. His

particular interests led him to an attack from the systems point of view.

Van der Pol was basically looking for a general analytical solution to his differential equation. To accomplish this he approximated the equation severely without regard to the possible ramifications of such approximations on a subtle phenomenon such as entrainment. He attacked the problem of modeling an oscillator from the straightforward network analysis point of view. He largely accomplished his objectives. The model derived was a good start but could not satisfactorily explain the details of synchronization.

Kurokawa attempted a middle course between Adler and van der Pol. He retained some form of nonlinearities and derived a bandwidth of synchronization. He also derived expressions for the steady state oscillation voltage. Kurokawa attacked the problem from the transformational and calculus of variation point of view. His approach is more complete than the others but it is also very hard to follow. The results are not intuitively simple or easy to assimilate.

4. OBJECTIVES

The effort expanded on theoretical modeling of the classical van der Pol or other phenomenological oscillator models is in stark contrast with the almost nonexistence of experimental studies involving real oscillator configurations. Such a real and practical oscillator will be the object of this study. This is a new and novel oscillator christened the Synchronous Oscillator by its discoverer Vasil Uzunoglu, a senior research specialist at Fairchild Industries [8].

As the name implies, the Synchronous Oscillator (SO) exhibits synchronization behavior that is both familiar and fascinating. The SO operates as a typical free-running oscillator when no signal is injected into it. The injection of a signal transforms the SO into a synchronization network. The SO behaves in the familiar way of frequency tracking of the injected signal at a constant phase. There are some unusual characteristics of the SO that go beyond the familiar synchronization behavior.

The curves of figure 4-1 show a standard synchronization response of the SO. The abscissa represents the frequency of the injected signal. The ordinate represents the magnitude of the frequency component within the output that is identical to the injected frequency. The ordinate also represents the phase

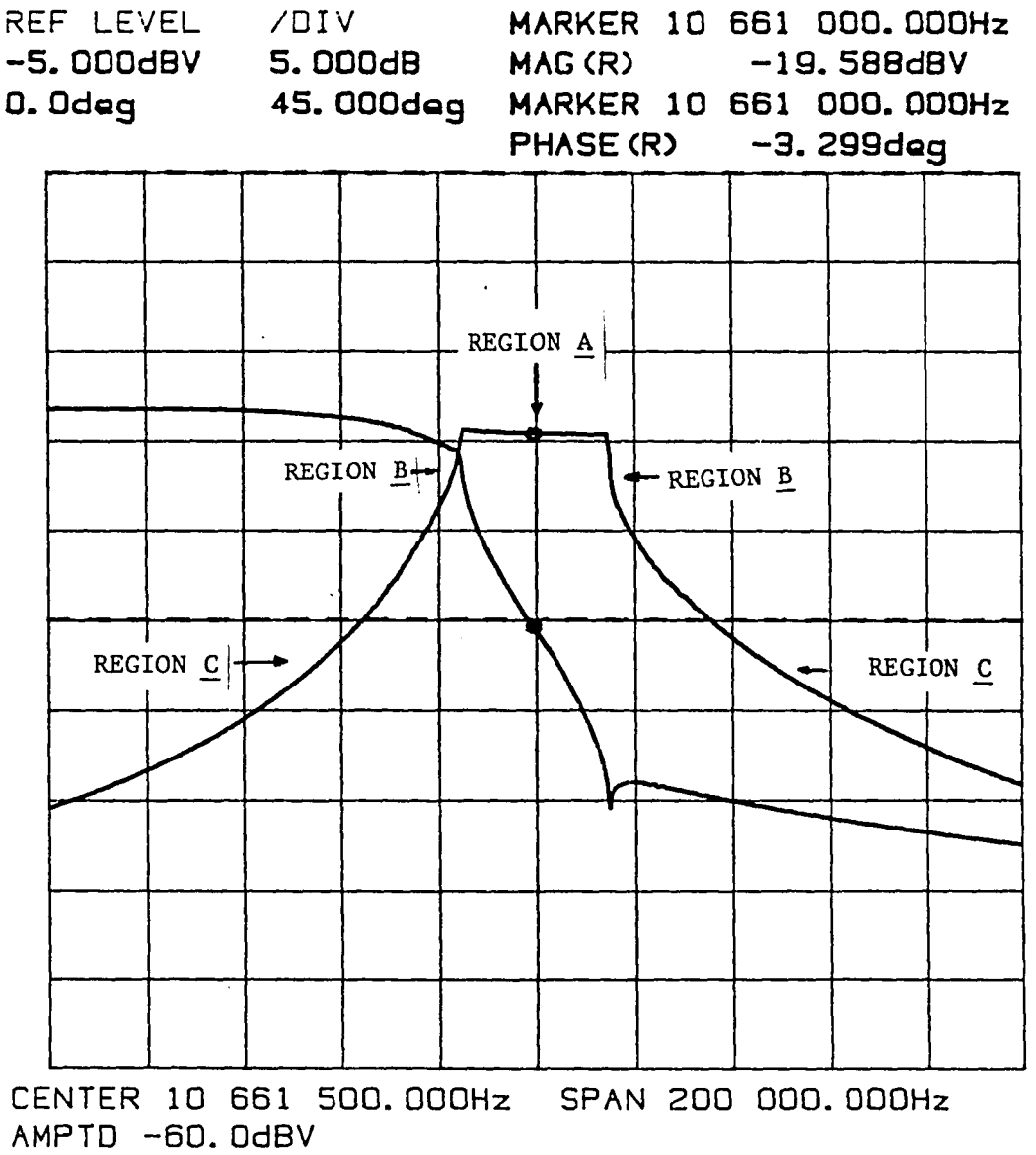

Figure 4-1: Phase-Gain plot of the SO. The abscissa represents frequency of injected signal. The ordinate represents the amplitude and phase of the oscillator.

difference between the injected signal and the output of the SO. The curves are produced with an HP 3577A network analyzer.

The figure can be divided into three regions. Region A represents the synchronization region. Here the magnitude of oscillation is invariant and the phase difference between the injected signal and the SO output is linear with respect to frequency. Region B represents a transition region characterized by very sharp skirt selectivity. The sharp skirts look almost like discontinuities. Regions C represent distorted oscillations with a very small component of the output at the injected frequency. Region A centers around the natural frequency of the oscillator. The width of region A is the familiar bandwidth of synchronization. This width has been found to be very sensitive to the magnitude of the injected signal [8]. An increase of the input magnitude results in the increase of the bandwidth. Figure 4-2 shows the dependence of bandwidth on the magnitude of the injected signal.

The synchronization curve of the SO is certainly unusual. The sharp corners and adaptive behavior of the bandwidth indicate important nonlinear mechanisms. No previous theoretical analysis has produced such a synchronization response. Van der Pol's solution in figure 3-1 cannot even begin to approximate the curves of figures 4-1 and 4-2. There are a few familiar characteristics within the SO curves. Region A is suggestive of the "phaselock" phenomenon and

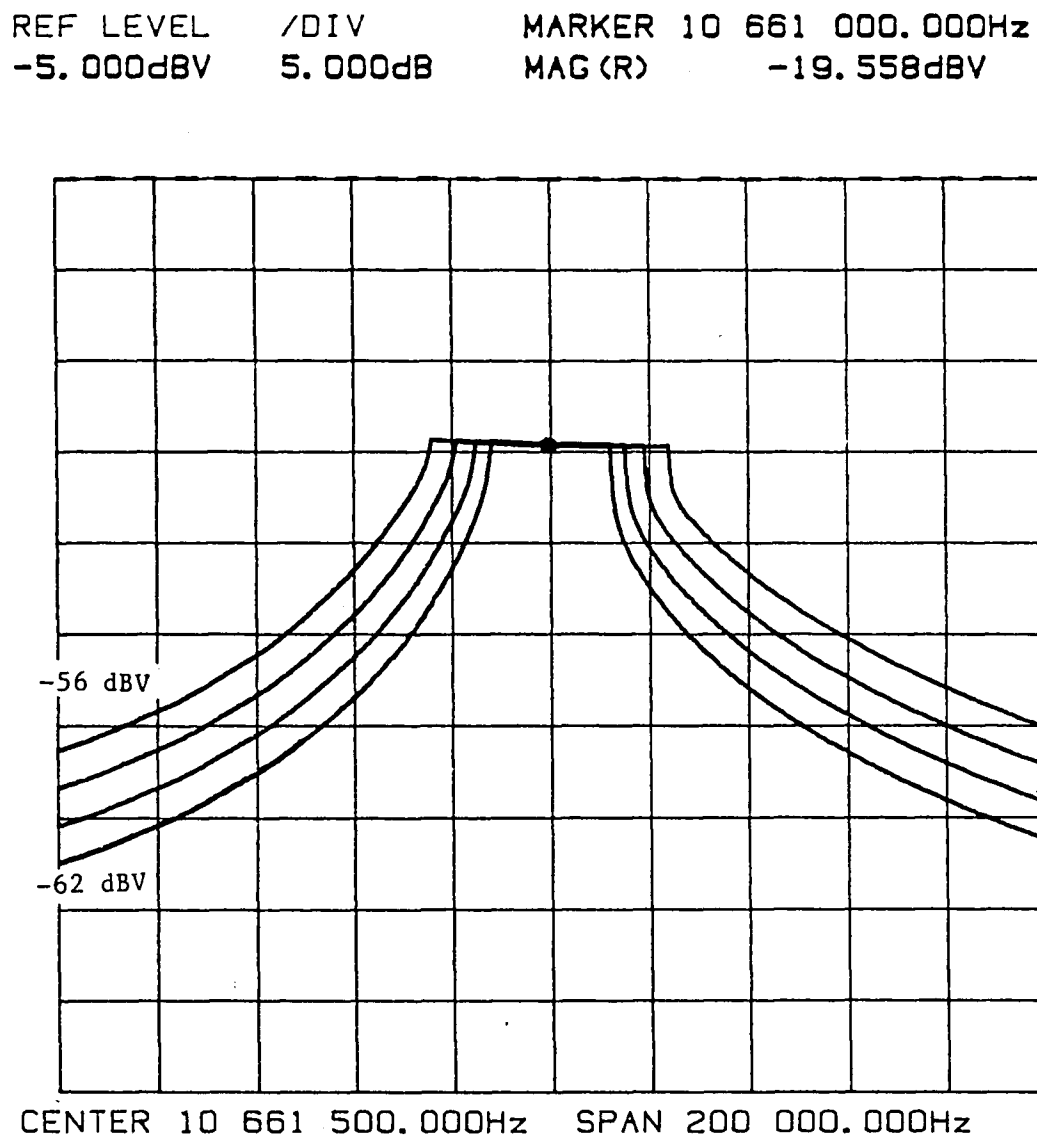

INJECTED SIGNAL AMPLITUDES: -56 dBV, -58 dBV, -60 dBV, -62 dBV.

Figure 4-2: Synchronization bandwidth dependance on the amplitude of the injected signal.

region C is reminiscent of the asynchronous quenching that Dewan tried to classify within the van der Pol solution. In the SO curves the phaselock and quenching regions are distinct and sharply defined. In the classical solution of figure 3-1 the regions are not intuitively distinct and rely on mathematical constructions such as saddle points and poles for definition [5]. The behavior of the SO in response to a change in injected magnitude also differs distinctly from the classical solution.

The SO curves may also seem familiar to Adler's analysis. Adler defined his synchronization region almost as if he had the SO in mind. The SO synchronization bandwidth is characterized by a constant amplitude and a linear phase difference with respect to frequency. This characterization also constitutes the founding assumption of Adler's analysis. Some of Adler's results do seem relevant to the SO. The expression for the synchronization bandwidth derived by Adler is proportional to the magnitude of the injected signal [6]. The SO shows similar dependence in Figure 4-2.

Adler's bandwidth is dependent on the transconductance of the active element in the oscillator. The analysis however says very little about the structure of this transconductance, which is a nonlinear unknown. Descriptions of this transconductance and the negative resistance that results from it have always been the weak point of any analysis of nonlinear oscillators.

Understanding the role played by the negative resistance in oscillators remains the only path not yet substantially explored. The goal of this study is the derivation of an expression for the nonlinear transconductance. The form of this expression is revealed through the observation of certain changes in the dc operating conditions within the SO circuit.

5. EXPERIMENTAL INVESTIGATION

The SO is a unique nonlinear oscillator capable of synchronization performance unmatched by any previous oscillator configuration. The unusual qualities of the SO are the driving force behind this investigation. A natural direction of inquiry is the development of a nonlinear model that can emulate the behavior of the real SO. It was made clear earlier in this study that a nonlinear analysis is the only route not substantially explored by researchers in the search for oscillator models.

Theoretical analysis of the SO cannot proceed without a basic physical understanding of the network. Figure 5-1 shows an oscillator that was constructed at Fairchild Laboratory of Lehigh University. This oscillator has a natural frequency of about 10 MHz. Figure 5-2 shows an oscillator that was assembled from parts provided by Fairchild Industries. This oscillator has a natural frequency of about 100 MHz.

There are basically two methods that are used at Fairchild Laboratory to probe the oscillators. The first and simpler method requires a large bandwidth oscilloscope such as the Tektronix 7854 with appropriate high impedance probes. This setup is useful in the observation of waveforms at various nodes of the SO. A more sophisticated method involves the use of a network analyzer such as

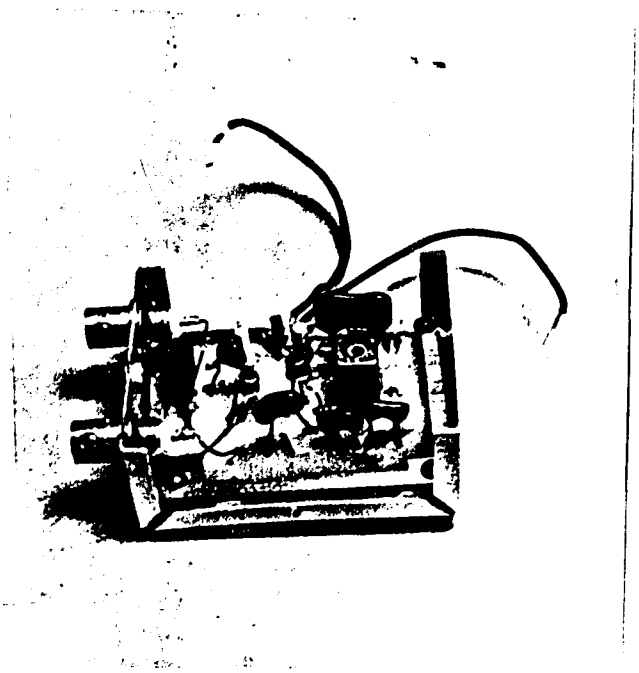

Figure 5-1: Oscillator built at Lehigh Univ.

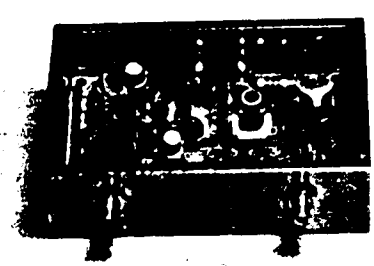

Figure 5-2: Oscillator assembled at Lehigh Univ. with parts provided by Fairchild Industries.

the HP 3577A. The analyzer is instrumental in the demonstration of synchronization behavior. The experimental setup of the network analyzer is shown in figure 5-3. A single frequency signal generated by the analyzer is injected into the SO. The frequency of the injected signal is swept by the analyzer between two limits that are set by the operator. The output of the SO is continuously monitored by the analyzer. The analyzer extracts from the SO output the frequency component that is identical to the frequency of the injected signal. This component is displayed on the screen of the analyzer.

A sample of experimental measurements with the network analyzer setup is shown in figure 5-4. The oscillator of figure 5-1 is used for these measurements. Notice the characteristic flat top and linear phase difference within the synchronization region. Adaptivity of the bandwidth of synchronization is displayed in figure 5-5. The change in bandwidth is due to a change of input signal magnitude.

The measurements obtained with the analyzer give insights and characteristics of the SO as a system. These measurements tell very little about the behavior of particular elements within the oscillator. To understand the inner workings of the SO an oscilloscope is indispensable. The oscilloscope probes the circuit at various points. Observation of waveforms at these points can

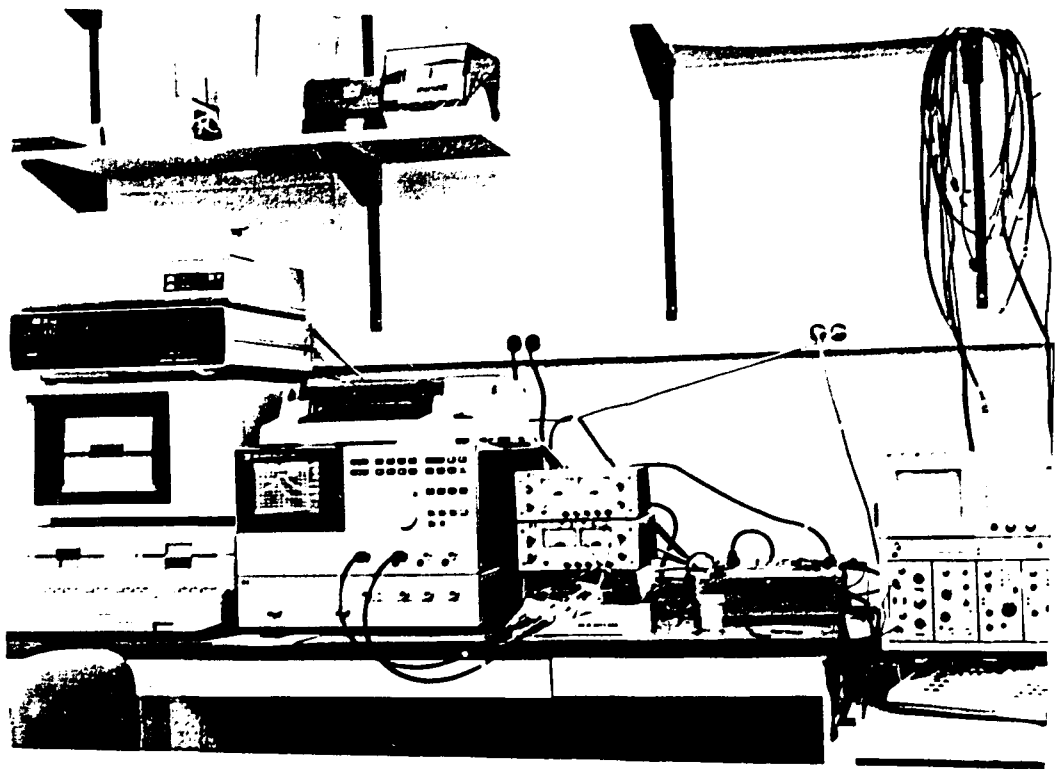

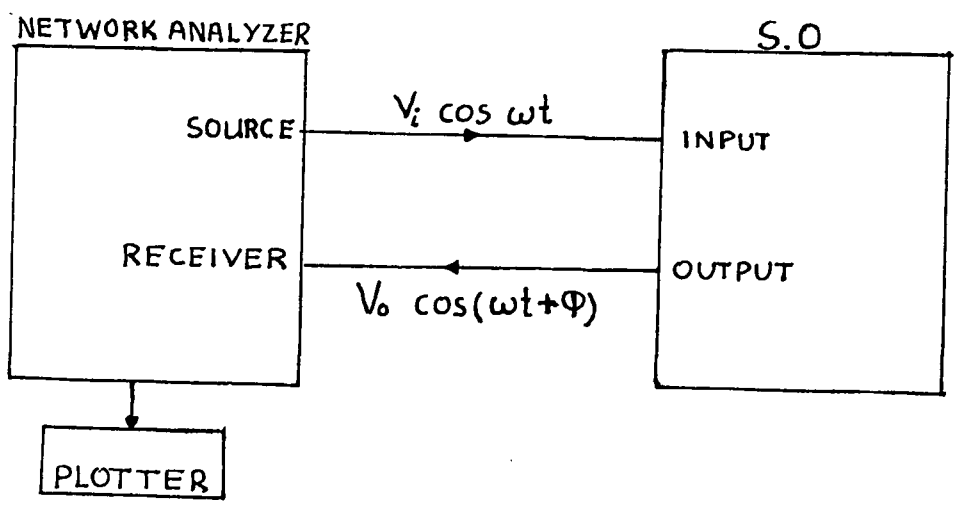

Figure 5-3: Scheme for Synchronization measurements using the network analyzer.

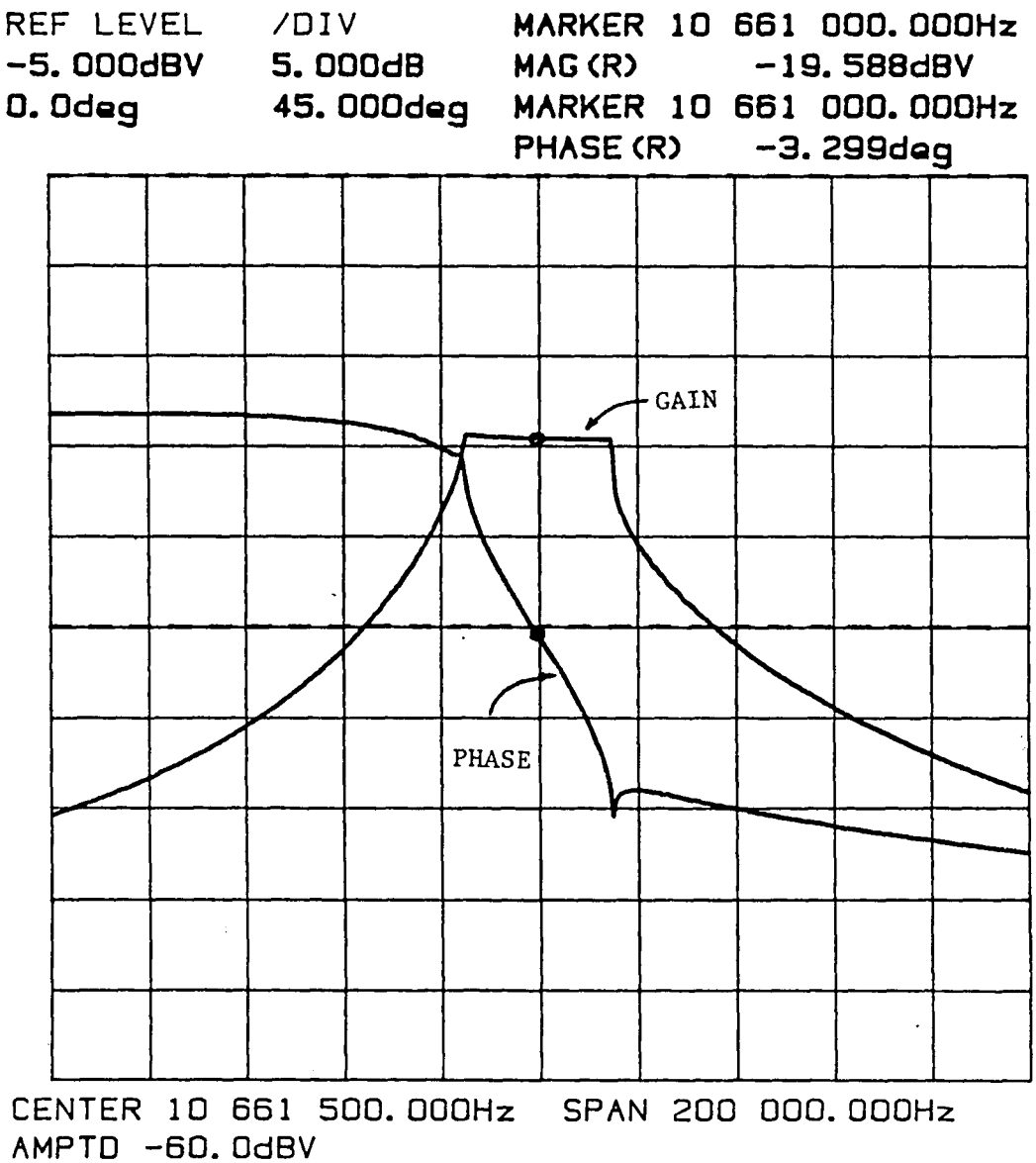

Figure 5-4: A Gain-Phase plot of the oscillator in figure 5-1.

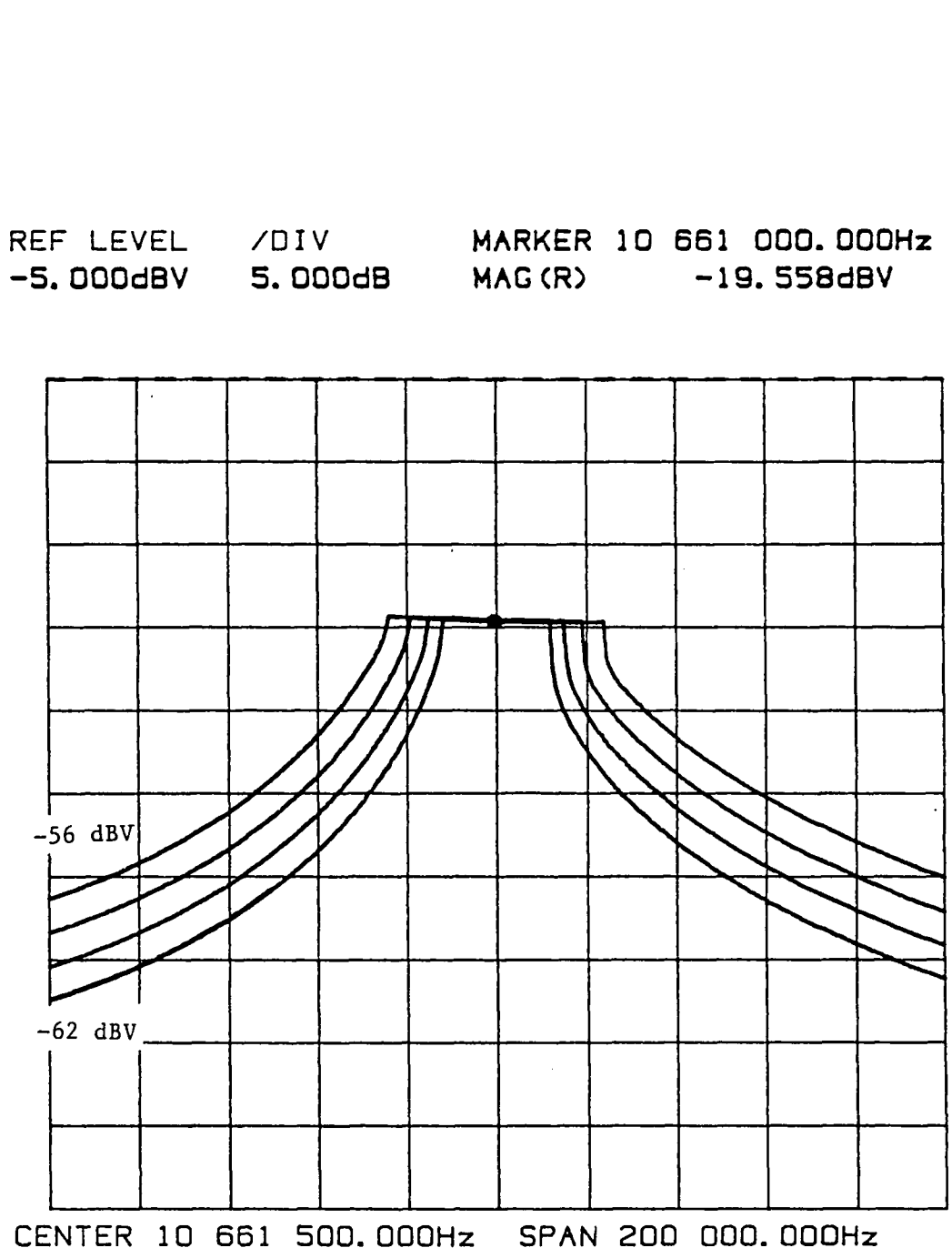

INJECTED SIGNAL AMPLITUDES: -56 dBV, -58 dBV, -60 dBV, -62 dBV.

Figure 5-5: Adaptivity of bandwidth due to changes in the amplitude of injected signal.

improve understanding and identify the elements that are important for the mathematical analysis.

The SO network is presented in figure 5-6. It is essentially a modified Colpitts oscillator. Bipolar transistor Q_1 is the oscillator transistor that is characterized by high frequency response and high gain, e.g. β=160. Bipolar transistor Q_2 is characteristically similar to Q_1 and performs two very important functions. First, it acts as a very high ac impedance from node 1 to ground. Second, Q_2 allows for the clean injection of an ac current into the high impedance node 1. It is clear this node is vitally important to the oscillator. The dc bias of the oscillator is adjusted via resistors R_1 and R_2 so that node 1 is at a dc operating point of about V_{C2}=1.5 volts with respect to ground.

A concrete understanding of the role played by Q_2 can be obtained by observing the I_{C2} vs V_{C2} characteristics of the transistor in figure 5-7. This characteristic is obtained via an HP 4145A Semiconductor Parameter Analyzer. The oscilloscope is used to probe node 1 of the oscillator in figure 5-6. Observation reveals a small (mV) ac signal riding on a 1.5 volt dc as indicated in figure 5-8. Notice that the oscillator is undriven during this experiment. Voltage V_{C2} of transistor Q_2 in figure 5-7 shows that for such an oscillation in voltage there is appreciable dc current (mA) but very little ac current (uA). The ac current is due to the "Early Effect"

THE SYNCHRONOUS OSCILLATOR

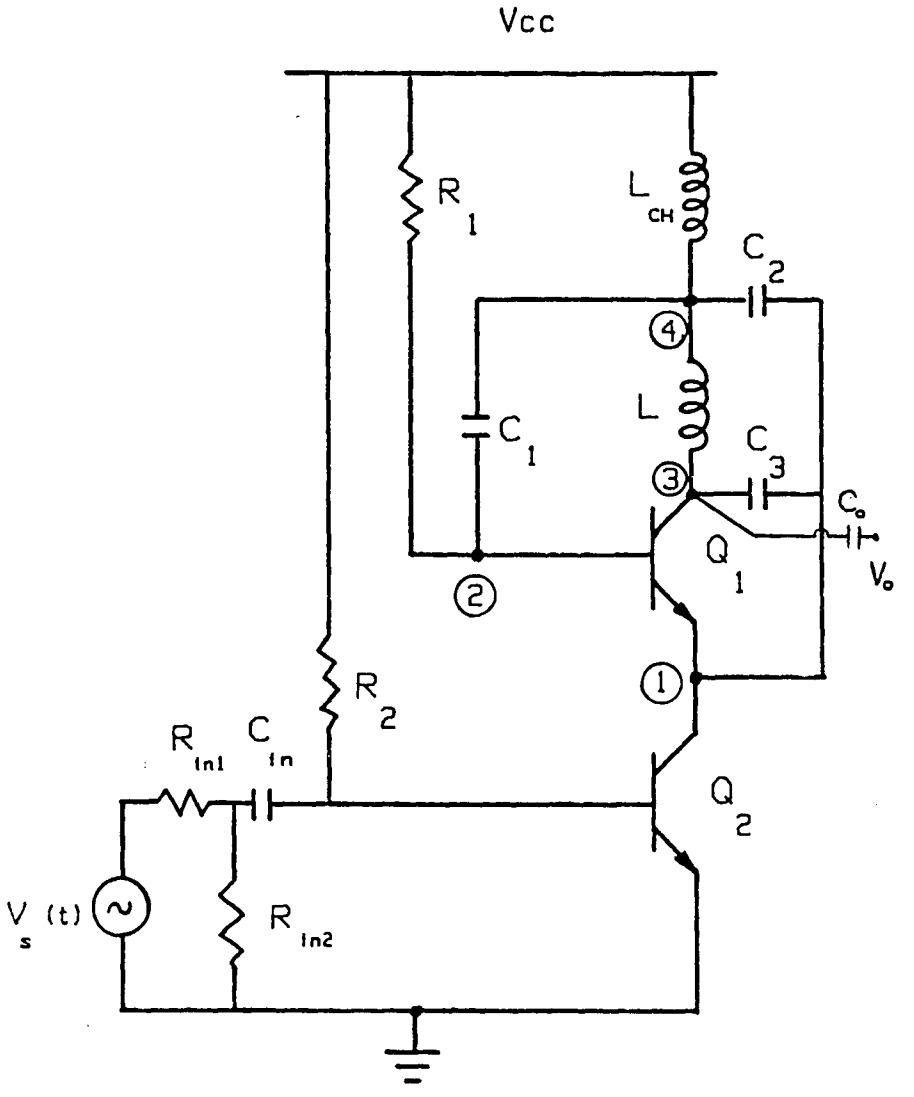

Figure 5-6: The Synchronous Oscillator circuit.

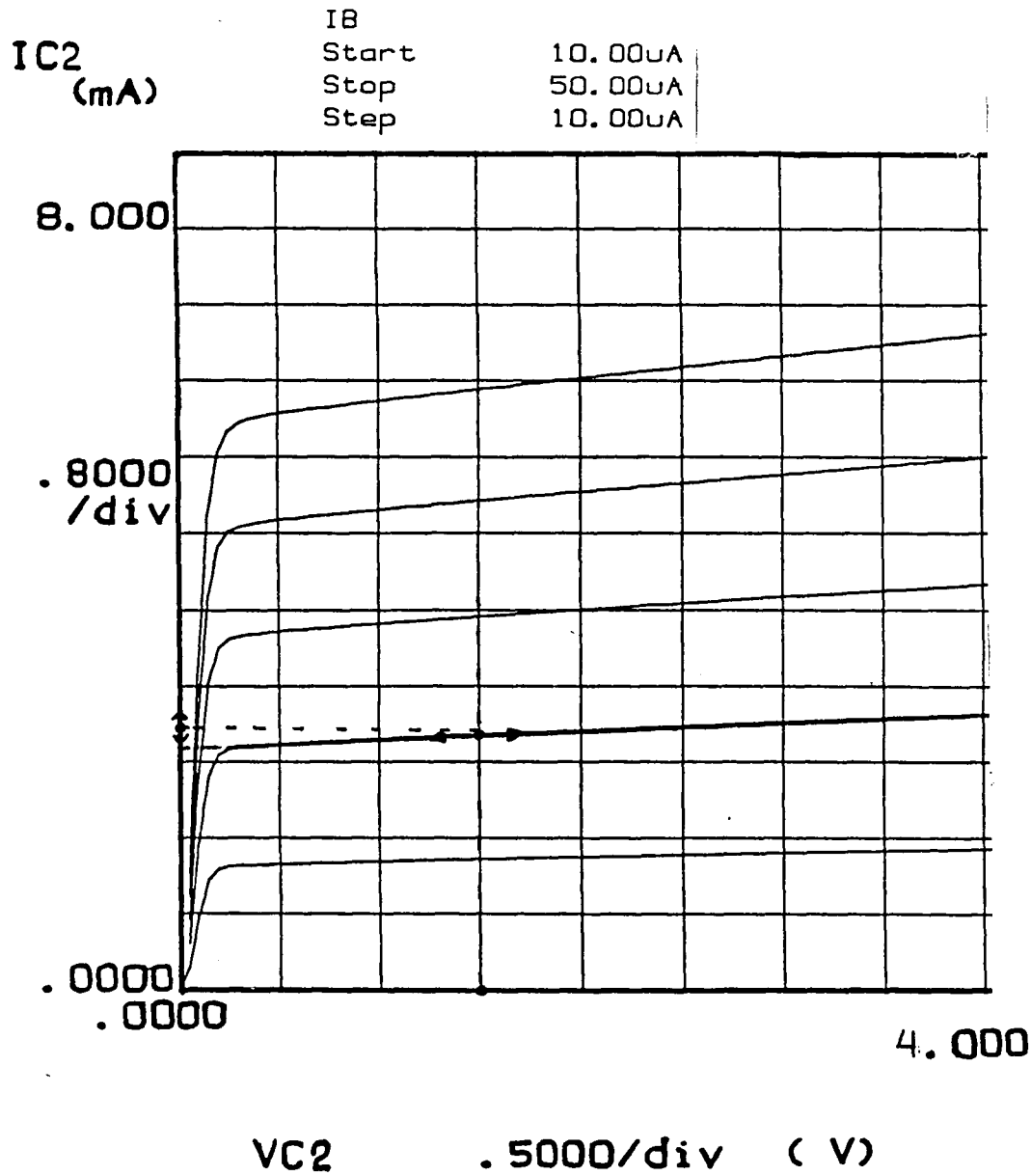

Figure 5-7: Collector current versus collector to emitter voltage of transistor Q_2.

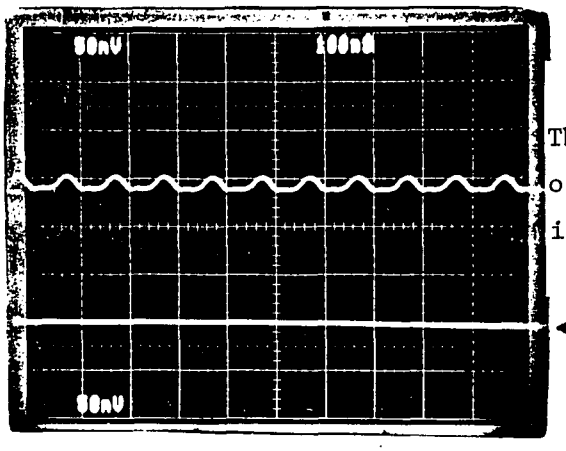

Figure 5-8: Oscilloscope probes node 1 of oscillator with 10X probe.

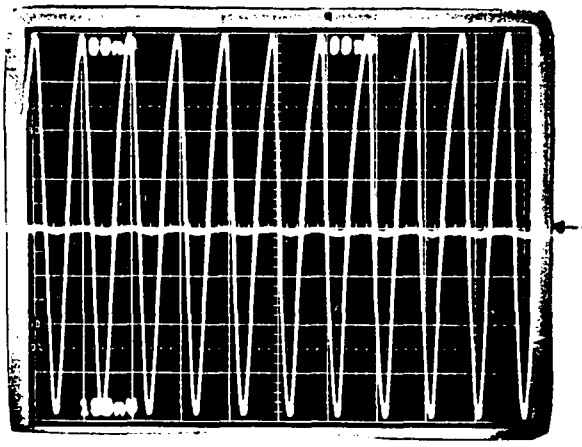

Figure 5-9: Sum and difference voltages from nodes 2 and 4.

conductance of the transistor. A small driving signal impressed on the base of Q_2 adds to the ac current a component $g_{m1}V_{b2}(t)$ where g_{m1} is the small signal transconductance of Q_2.

Further examination of the circuit in figure 5-6 reveals two feedback paths. One feedback connects node 4 to the base of Q_1 via the large capacitor C_1. This capacitor acts as an ac short between the two nodes. The second feedback comes from the resonating tank into node 1. The evidence of an ac short across C_1 comes from probing nodes 2 and 4. Figure 5-9 compares the sum and difference of the ac voltages at the two nodes with respect to ground. The difference is practically zero when compared to the sum.

Observations of the voltage $v_{B1}(t)$ across the base-emitter junction of transistor Q_1 reveal an important attribute of the SO. Transistor Q_1 is operating in class C mode. Figure 5-10 indicates the operation is characterized by a base-emitter junction which is reverse biased for a major part of each cycle of oscillation. The collector current of Q_1 is released in bursts as the base-emitter junction becomes forward biased. The class C operation forces the dc operating point of $v_{B1}(t)$ to become negative. As the peak to peak magnitude of $v_{B1}(t)$ changes, the operating point also changes.

The crests of the oscillation $v_{B1}(t)$ are pinned at the rectification voltage of about .7 volts. The troughs of the

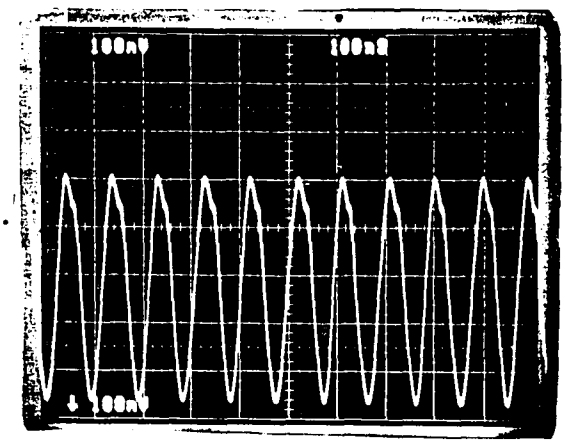

Figure 5-10: The base-emitter voltage of transistor Q_1.

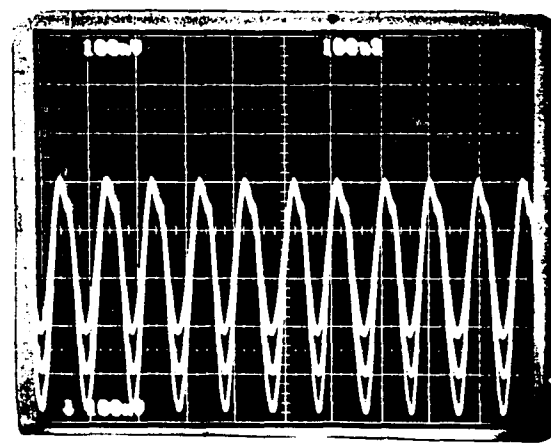

Figure 5-11: Voltage across base-emitter junction of Q_1 for different magnitudes of oscillation.

oscillation change when the peak to peak magnitude of $v_{B1}(t)$ changes. Figure 5-11 demonstrates the phenomenon. When the peak to peak magnitude becomes less than twice the rectification limit, the operating point becomes positive, indicating class A operation. The conclusion is that the oscillating transistor Q_1 adopts class A, B or C mode of operation depending on the peak to peak magnitude of $v_{B1}(t)$. The voltage $v_{B1}(t)$ can be modeled by

$$v_{B1}(t) = V_{B1} + v_{b1}(t)$$

with

$$v_{b1}(t) = V\cos \omega t$$

The phenomenon of varying operating point will become of central concern during the mathematical analysis of the SO.

6. THEORETICAL ANALYSIS

Basic observations about the behavior of the voltage $v_{B1}(t)$ across the base-emitter junction of Q_1 hold the key to a sucessful understanding of the prevailing dc operating conditions within the SO. The fundamental clue used in this mathematical treatment is the fact that Q_1 is operating in class C mode.

Removal of feedback capacitor C_1 in figure 5-6 causes oscillations to stop. Figure 6-1 shows the dc paths of the non-oscillating circuit. Currents I_{C1} and I_{C2} may be easily obtained by summation of currents flowing into node 1. Current I_{C2} is

$$I_{C2} = I_{S2}\, e^{\alpha V_{B2}} = \frac{(V_{CC} - V_{B2})}{R_2}\left(1 + \frac{V_{C2}}{V_A}\right)\beta_2 \qquad (6.1)$$

The early voltage V_A of Q_2 is about 120 volts neglecting the conductance term. Notice that I_{C2} is defined by physical parameters such as I_{S2}, R_2, V_{CC} and the gain of Q_2. Similarly the current I_{C1} may be expressed as

$$\bar{I}_{C1} = I_{S1}\, e^{\alpha \bar{V}_{B1}} = \frac{(V_{CC} - \bar{V}_{B1} - V_{C2})}{R_1}\,\beta_1 \qquad (6.2)$$

where $\bar{V}_{B1}$ is the "rectification" voltage across the base-emitter junction of Q_1 (about .7 volts). Realizing that

THE SYNCHRONOUS OSCILLATOR

DC CIRCUIT

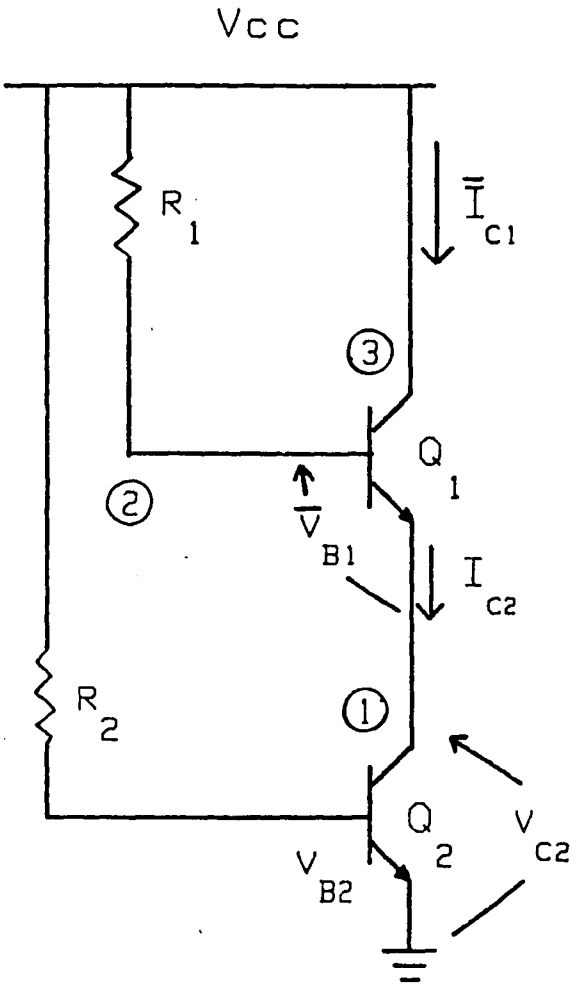

Figure 6-1: The dc paths of the non-oscillating circuit.

$$I_{C2} = \bar{I}_{C1} + \frac{(V_{CC} - \bar{V}_{B1} - V_{C2})}{R_1} \qquad (6.3)$$

allows for the expression of V_{C2} as

$$V_{C2} = (V_{CC} - \bar{V}_{B1}) - \frac{R_1\beta_2}{R_2\beta_1}(V_{CC} - V_{B2}) \qquad (6.4)$$

The above equations define the dc currents and voltages of the non-oscillating circuit in terms of known quantities.

The introduction of capacitor C_1 back into the circuit results in the resumption of stable oscillation. Reexamination of the dc component of $v_{B1}(t)$ reveals that it is not .7 volts. We observe that

$$V_{B1} < \bar{V}_{B1} = .7 \text{ Volts} \qquad (6.5)$$

Consequently the dc current through the collector of Q_1 should be less than $\bar{I}_{C1}$. Let us denote a new dc current I_{C1} that corresponds to the case where $V_{B1} < .7$ volts. Figure 6-2 shows the dc voltages and currents for the oscillating circuit. Now, summing currents at node 1 yields

$$I_{C2} = I_{C1} + \frac{(V_{CC} - V_{B1} - V_{C2})}{R_1} \qquad (6.6)$$

Substitution for I_{C2} into equation (6.3) yields

THE SYNCHRONOUS OSCILLATOR

DC CIRCUIT

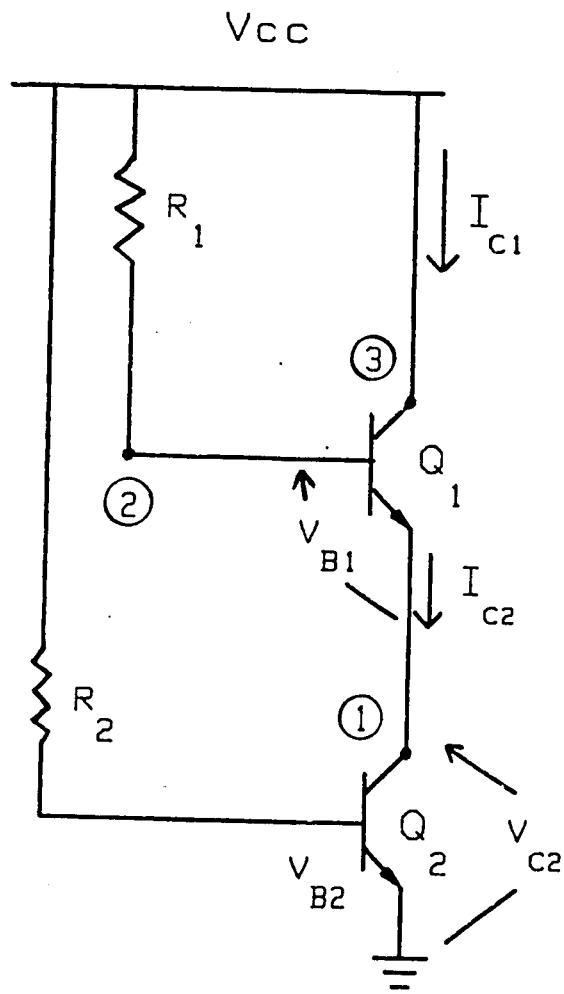

Figure 6-2: The dc paths for oscillating circuit.

$$\bar{I}_{C1} + \frac{(V_{CC} - \bar{V}_{B1} - V_{C2})}{R_1} = I_{C1} + \frac{(V_{CC} - V_{B1} - V_{C2})}{R_1} \qquad (6.7)$$

where I_{C2} remains the constant, independent of the existence of oscillations. Finally

$$\bar{I}_{C1} - \frac{\bar{V}_{B1}}{R_1} = I_{C1} - \frac{V_{B1}}{R_1} \qquad (6.8)$$

where

$$\bar{I}_{C1} = I_{S1} e^{\alpha \bar{V}_{B1}} \qquad (6.9)$$

Equation (6.8) relates the oscillatory dc collector current I_{C1} to the dc base-emitter voltage V_{B1} of Q_1.

Another expression for I_{C1} in terms of V_{B1} can make equation (6.8) very useful in subsequent analysis. Toward this end, it was pointed out earlier that during oscillation the voltage $v_{B1}(t)$ across the base-emitter junction of Q_1 is

$$v_{B1}(t) = V_{B1} + v_{b1}(t) \qquad (6.10)$$

where

$$v_{b1}(t) = V\cos \omega t \qquad (6.11)$$

The collector current induced in Q_1 due to this junction voltage is

$$i_{C1}(t) = I_{S1} e^{\alpha v_{B1}(t)} = I_{S1} e^{\alpha (V_{B1} + v_{b1}(t))} \qquad (6.12)$$

The time varying exponential may be expanded into a series of harmonics. If only the dc and fundamental harmonics are retained, $i_{C1}(t)$ may be expressed as

$$i_{C1}(t) = I_{S1} e^{\alpha V_{B1}} \left(I_0(\alpha V) + \alpha I_{02}(\alpha V) v_{b1}(t) \right) \qquad (6.13)$$

where

$$I_0(\alpha V) = \sum_{n=0}^{\infty} \left(\frac{\alpha V}{2}\right)^{2n} \frac{1}{(n!)^2} \qquad (6.14)$$

and

$$I_{02}(\alpha V) = I_0(\alpha V) - I_2(\alpha V) = \sum_{n=0}^{\infty} \left(\frac{\alpha V}{2}\right)^{2n} \frac{1}{n!(n+1)!} \qquad (6.15)$$

The functions $I_0(\alpha V)$ and $I_{02}(\alpha V)$ are modified Bessel functions. Appendix I provides a detailed account of the derivation for $i_{C1}(t)$. Now it becomes apparent that $v_{B1}(t)$ produces a dc component of $i_{C1}(t)$ that may be expressed as

$$I_{C1} = I_{S1} e^{\alpha V_{B1}} I_0(\alpha V) \qquad (6.16)$$

while the ac component may be expressed as

$$i_{c1}(t) = \alpha I_{S1} e^{\alpha V_{B1}} I_{02}(\alpha V)\, v_{b1}(t) \qquad (6.17)$$

Substitution of I_{C1} into equation (6.8) yields

$$I_{S1} e^{\alpha \bar{V}_{B1}} - \frac{\bar{V}_{B1}}{R_1} = I_{S1} e^{\alpha V_{B1}} I_0(\alpha V) - \frac{V_{B1}}{R_1} \qquad (6.18)$$

Transcendental equation (6.18) indicates a relation between the dc and ac magnitudes of $v_{B1}(t)$. Simplification of this equation yields

$$I_{S1} e^{\alpha \bar{V}_{B1}} = I_{S1} e^{\alpha V_{B1}} I_0(\alpha V) \qquad (6.19)$$

which results in

$$\bar{V}_{B1} - V_{B1} = \frac{\ell n\, [I_0(\alpha V)]}{\alpha} \qquad (6.20)$$

Notice that as oscillations stop, V--> 0 and V_{B1}--> $\bar{V}_{B1}$. This relation is observed experimentally as shown in figure 5-11. Now let us define G_m from equation (6.17) as

$$G_m = \frac{i_{c1}(t)}{v_{b1}(t)} = \alpha I_{S1} e^{\alpha V_{B1}} I_{02}(\alpha V) \qquad (6.21)$$

If equation (6.19) is substituted for V_{B1} in (6.21), G_m can be expressed as

$$G_m = \alpha I_{S1} \, e^{\alpha \bar{V}_{B1}} \frac{I_{02}(\alpha V)}{I_0(\alpha V)} \qquad (6.22)$$

Simplified versions of G_m are derived in appendix II. Finally, the simplest way that G_m can be modeled is

for $V < (2/\alpha)$ $$\bar{\bar{G}}_m = g_{m1} = \alpha I_{S1} \, e^{\alpha \bar{V}_{B1}} = \frac{q}{kT} \bar{I}_{C1} \qquad (6.23)$$

and

for $V > (2/\alpha)$ $$\bar{\bar{G}}_m = g_{m1} \left(\frac{2}{\alpha V}\right)$$

as illustrated in figure (6-3).

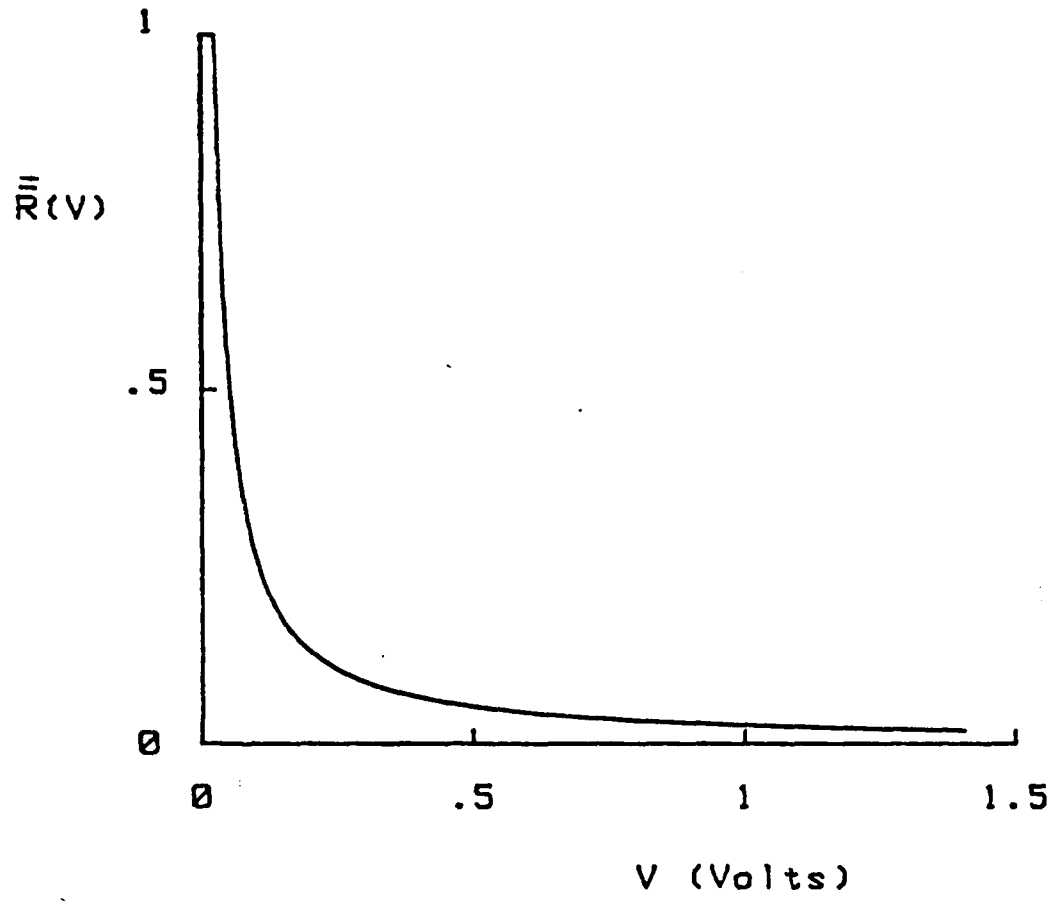

Figure 6-3: $\bar{\bar{R}}(V)$ is the ratio $\bar{\bar{G}}_m/g_{m1}$.

7. CONCLUSION

Research literature devoted to the study of synchronization in nonlinear oscillators is very limited. The literature that does deal with synchronization is predominantly phenomenological in the structure of its analyses. Analytical models of synchronization based on actual oscillator circuits are almost nonexistent. The cause of the scarcity of models can be traced to difficulties in treating nonlinear quantities in these oscillator circuits. Such nonlinear quantities are frequently lumped into a single term called the negative resistance. Lack of knowledge about negative resistance is the prime impediment to further progress in modeling synchronization. The focus of this study was to give some form to the elusive negative resistance.

The object of the study was a novel type of network called the Synchronous Oscillator (SO). The structure of this oscillator lends itself easily to an analytical attempt toward unraveling the form of the negative resistance. In the SO, nonlinear resistance comes in the guise of a nonlinear transconductance (G_m) of a transistor. The analysis in chapter 6 yielded an expression for the G_m that is intuitively simple and consistent with the small signal g_m of a transistor.

The G_m is a function of the amplitude of oscillation. Small

oscillations show G_m to be equal to the widely known small signal g_m.

$$g_m = \frac{q}{kT} I_C$$

Large oscillations force the G_m to decrease inversely proportional to the amplitude of oscillation. This decrease in G_m explains the fact that the oscillator eventually must reach steady state. Adler explains [6] that the G_m must decrease until it just cancels out the resistive losses in the oscillator, at which point steady state is achieved.

The derived G_m can now be used in an ac analysis to ascertain three expressions:

1. An expression can be derived that predicts the magnitude of oscillations in the Synchronous Oscillator.
2. An expression must be derived that shows the magnitude of oscillation as a function of an injected input.
3. The transfer function in 2 must be used to obtain an expression of the bandwidth as a function of the input magnitude.

These issues provide ample material for future investigation. These and other issues pertinent to synchronization in Synchronous Oscillators are briefly illustrated in appendix III.

I. EXPANSION OF COLLECTOR CURRENT AS A HARMONIC SERIES

Given the current $i_{C1}(t)$,

$$i_{C1}(t) = I_{S1}\, e^{\alpha V_{B1}} \sum_{n=0}^{\infty} \frac{\left(\alpha v_{b1}(t)\right)^n}{n!} \qquad (I.1)$$

where

$$v_{b1}(t) = V \cos \omega t \qquad (I.2)$$

the formulas needed to transform powers of a cosine function into series of harmonics are:

for odd powers,

$$\cos^{2n-1}\omega t = \frac{1}{2^{2(n-1)}} \left\{ \cos(2n-1)\omega t + \begin{bmatrix} 2n-1 \\ 1 \end{bmatrix} \cos(2n-3)\omega t + \ldots + \begin{bmatrix} 2n-1 \\ 1 \end{bmatrix} \cos \omega t \right\} \qquad (I.3)$$

for even powers

$$\cos^{2n}\omega t = \frac{1}{2^{2n}} \begin{bmatrix} 2n \\ n \end{bmatrix} + \frac{1}{2^{2n-1}} \left\{ \cos 2n\omega t + \begin{bmatrix} 2n \\ 1 \end{bmatrix} \cos(2n-2)\omega t + \ldots + \begin{bmatrix} 2n \\ n-1 \end{bmatrix} \cos 2\omega t \right\} \qquad (I.4)$$

where

$$\begin{bmatrix} n \\ k \end{bmatrix} = \frac{n!}{k!(n-k)!} \qquad (I.5)$$

Observe that the odd powers of the cosine contribute only to the odd harmonics and the even powers contribute only to the even harmonics. As pointed out earlier in this study, the dc and fundamental frequency terms are sufficient for this analysis.

Each even power $\cos^{2n}\omega t$ contributes

$$\frac{1}{2^{2n}} \begin{bmatrix} 2n \\ n \end{bmatrix} \qquad (I.6)$$

to the dc term of the current $i_{C1}(t)$. Each odd power $\cos^{2n-1}\omega t$ contributes

$$\frac{1}{2^{2(n-1)}} \begin{bmatrix} 2n-1 \\ n-1 \end{bmatrix} \cos \omega t \qquad (I.7)$$

to the fundamental frequency term of $i_{C1}(t)$. Separation of the odd and even terms within the collector current (I.1) results in

$$i_{C1}^{even}(t) = I_{S1} e^{\alpha V_{B1}} \sum_{n=0}^{\infty} \frac{(\alpha V)^{2n}}{(2n)!} \cos^{2n} \omega t \qquad (I.8)$$

and

$$i_{C1}^{odd}(t) = I_{S1}\, e^{\alpha V_{B1}} \sum_{n=1}^{\infty} \frac{(\alpha V)^{2n-1}}{(2n-1)!} \cos^{2n-1} \omega t \qquad (I.9)$$

Now if the $\cos^{2n-1}\omega t$ in (I.9) is replaced by (I.7), the fundamental frequency component of $i_{C1}(t)$ can be written as

$$i_{c1}(t) = I_{S1}\, e^{\alpha V_{B1}}{}_{\alpha}\, v_{b1}(t) \sum_{n=0}^{\infty} \left(\frac{\alpha V}{2}\right)^{2n} \frac{1}{n!(n+1)!} \qquad (I.10)$$

If the $\cos^{2n}\omega t$ in (I.8) is replaced by the term (I.6), the dc component of $i_{C1}(t)$ can be written as

$$I_{C1} = I_{S1}\, e^{\alpha V_{B1}} \sum_{n=0}^{\infty} \frac{(\alpha V)^{2n}}{2^{2n}(n!)^2} \qquad (I.11)$$

where

$$I_0(\alpha V) = \sum_{n=0}^{\infty} \left(\frac{\alpha V}{2}\right)^{2n} \frac{1}{(n!)^2} \qquad (I.12)$$

and

$$I_{02}(\alpha V) = I_0(\alpha V) - I_2(\alpha V) = \sum_{n=0}^{\infty} \left(\frac{\alpha V}{2}\right)^{2n} \frac{1}{n!(n+1)!} \qquad (I.13)$$

II. SIMPLIFICATION OF NONLINEAR TRANSCONDUCTANCE

It has been established that

$$G_m = \alpha I_{S1} \, e^{\alpha V_{B1}} \, I_{02}(\alpha V) \tag{II.1}$$

and that

$$\bar{V}_{B1} - V_{B1} = \frac{\ln[I_0(\alpha V)]}{\alpha} \tag{II.2}$$

The transconductance can be expressed as

$$G_m = g_{m1} \, R(V) \tag{II.3}$$

where

$$g_{m1} = \alpha I_{S1} \, e^{\alpha \bar{V}_{B1}} = \alpha \bar{I}_{C1} \tag{II.4}$$

and

$$R(V) = \frac{I_{02}(\alpha V)}{I_0(\alpha V)} \tag{II.5}$$

The central focus of this appendix is the development of a simple expression to replace the function R(V). Figure (II-1) illustrates the form of R(V). Notice that for large V, R(V)~1/V, while for V-->0, R(V)-->1. A simple function that exhibits similar behavior

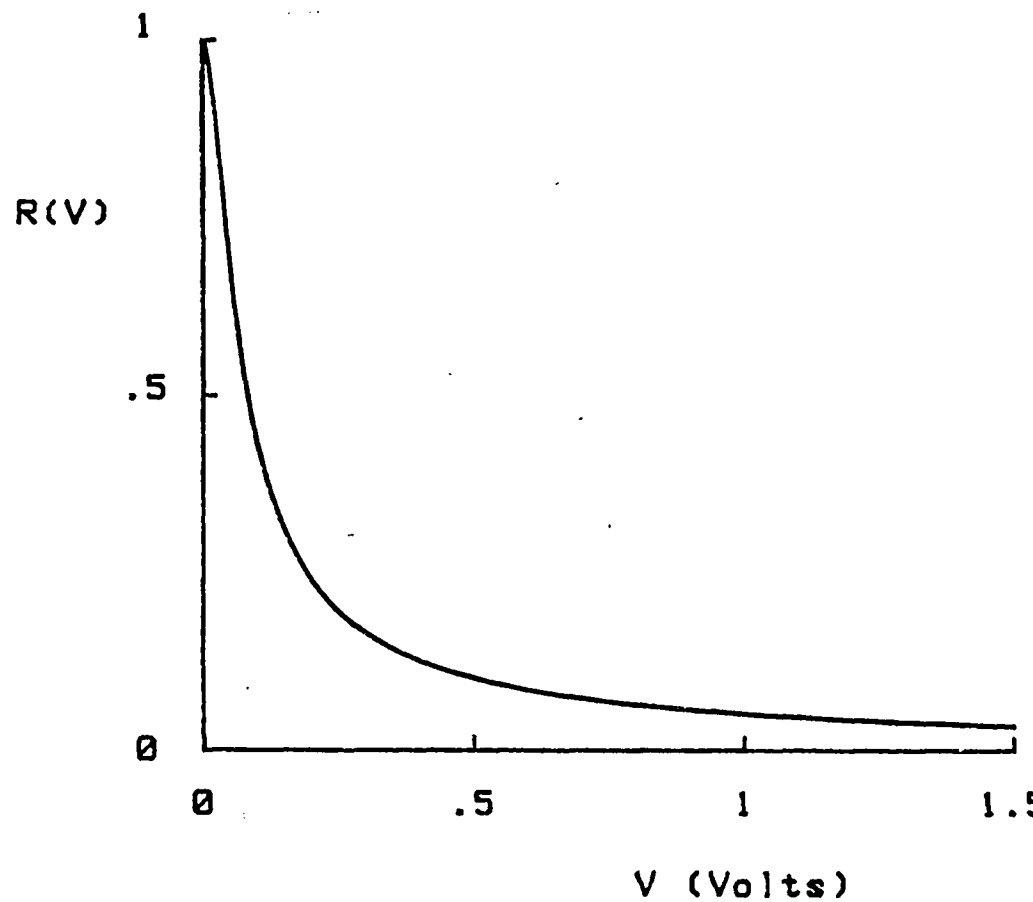

Figure II-1 The function R(V) decreases as $2/\alpha V$ for large V.

is

$$\bar{R}(V) = \frac{2}{\alpha V}\left[1 - e^{-\left(\frac{\alpha V}{2}\right)}\right] \qquad \text{(II.6)}$$

and is plotted in figure (II-2). In turn the expression for $\bar{R}(V)$ can be simplified further to a piecewise continuous form if it is assumed that 1/e is approximately zero.

$$\bar{\bar{R}}(V) = U(\frac{2}{\alpha} - V) + \frac{2}{\alpha V} U(V - \frac{2}{\alpha}) \qquad \text{(II.7)}$$

The above equation (II.7) is plotted in figure (II-3). Using this simple expression I define a simplified transconductance.

$$\bar{\bar{G}}_m = g_{ml} \bar{\bar{R}}(V) \qquad \text{(II.8)}$$

This is the final form for G_m.

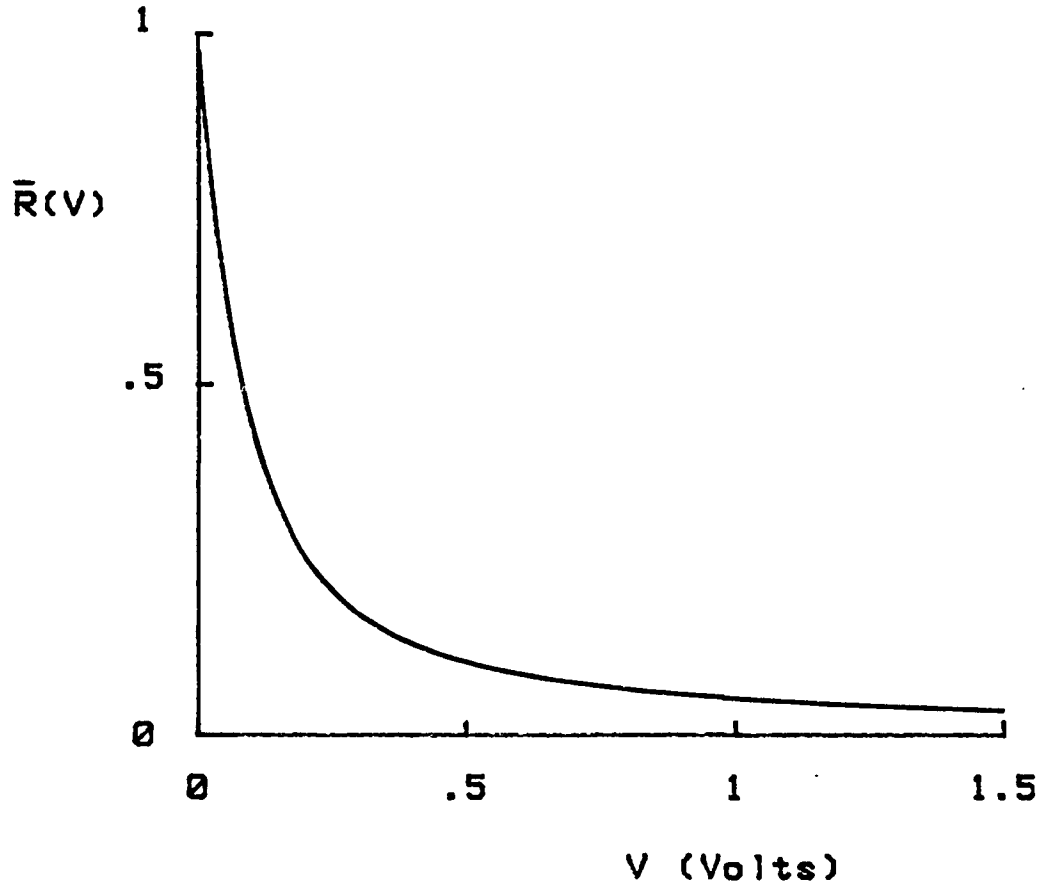

Figure II-2 This is a continuous approximation of the function R(V).

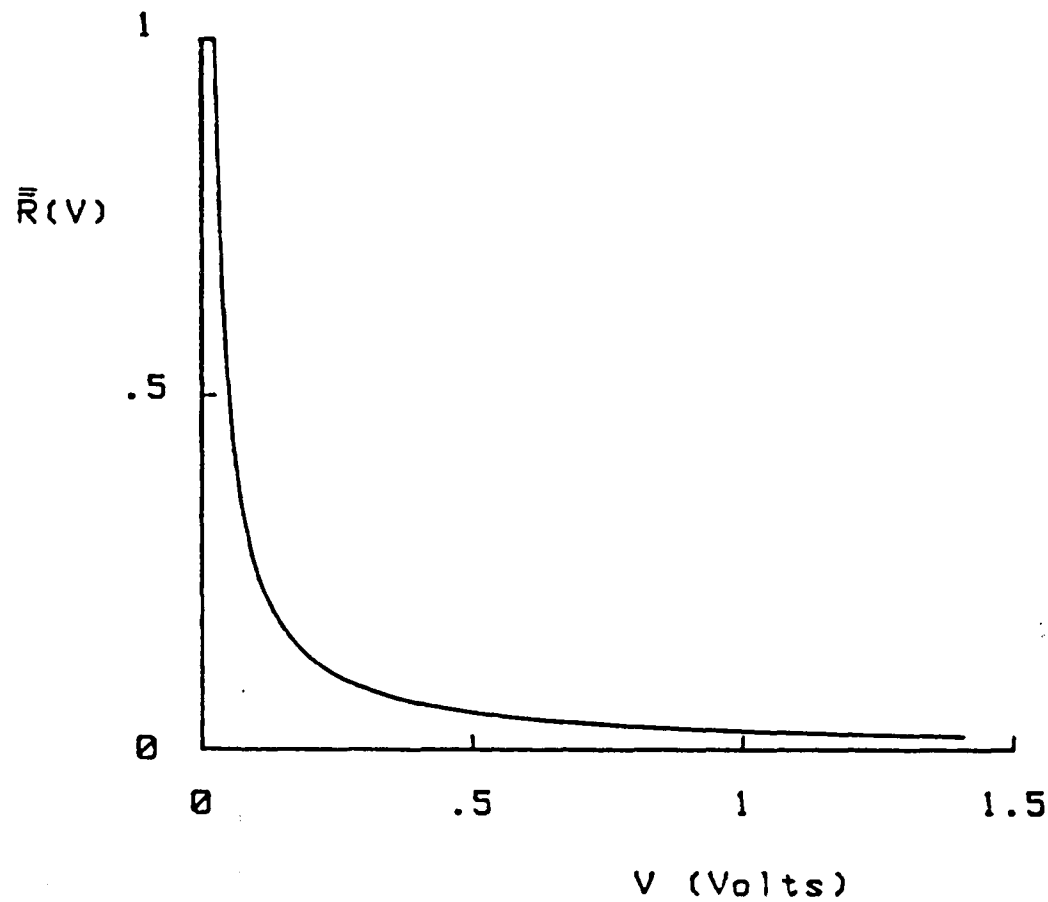

Figure II-3 This is a piecewise continuous approximation of the function R(V).

III. INTRODUCTION TO THE THEORY OF SYNCHRONOUS OSCILLATORS

This appendix represents a technical presentation given at Fairchild Industries on November 30, 1984. The author is my advisor Dr. Marvin H. White, endowed professor at the Fairchild Center for Solid State Studies of Lehigh University. The presentation summarizes Dr. White's results from a linear analysis of the various open issues in the theory of the Synchronous Oscillator. This linear analysis forms the basis for subsequent nonlinear analysis to be done using the nonlinear transconductance derived in this study.

OUTLINE

(1) INTRODUCTION
   (A) FUNCTIONAL DESCRIPTION
   (B) NONLINEAR OPERATION
(2) LINEAR ANALYSIS
(3) PHASE MODULATION
   (A) DRIVEN AND UNLOCKED
   (B) DRIVEN AND LOCKED (SYNCHRONIZED)
(4) ADAPTIVE 'TRACKING' BANDWIDTH
(5) PHASE ACQUISITION
(6) HARMONIC PUMPING
(7) CONCLUSIONS

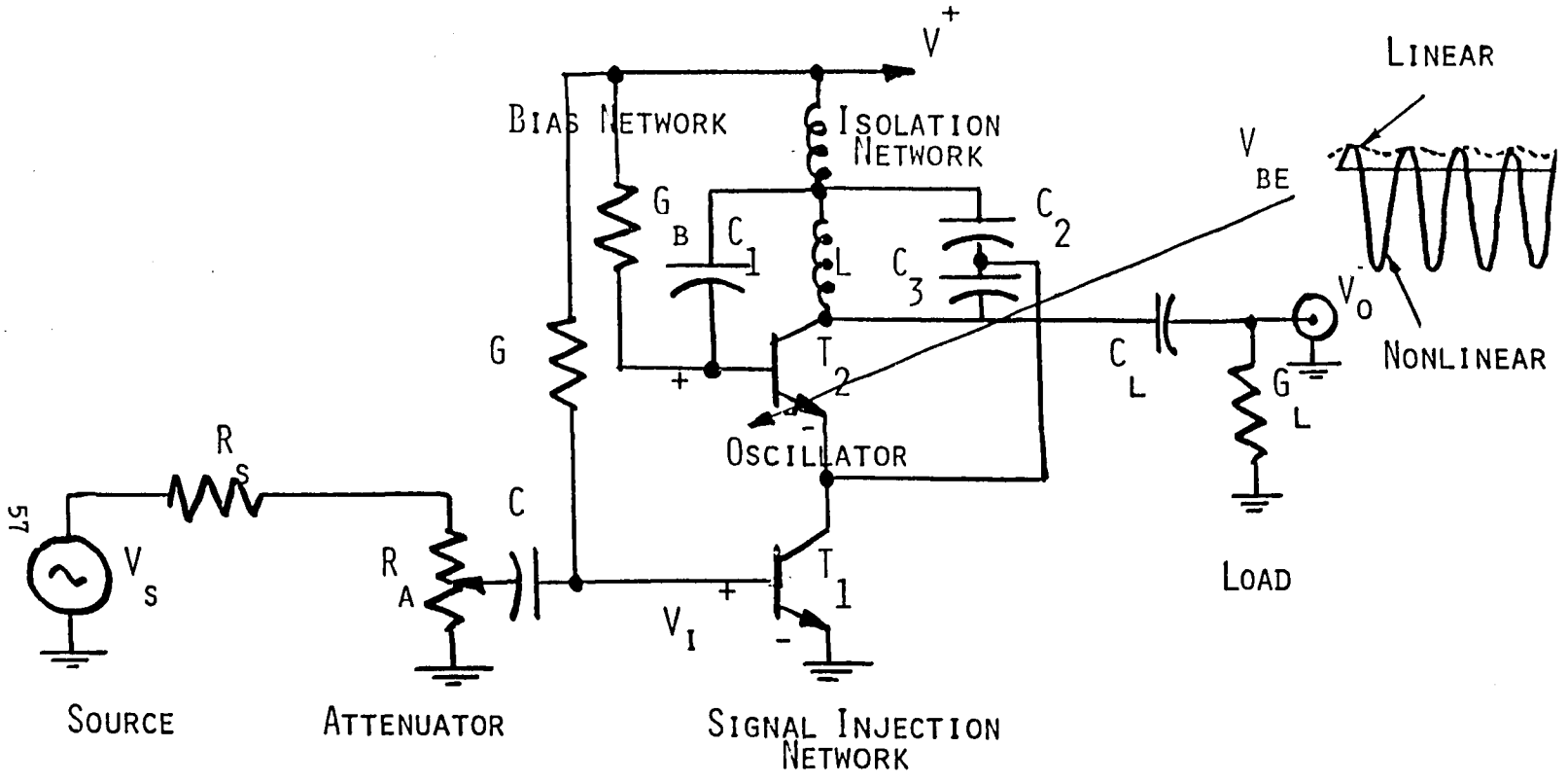

FUNCTIONAL DESCRIPTION OF
THE SYNCHRONOUS OSCILLATOR CIRCUIT

Linear Analysis

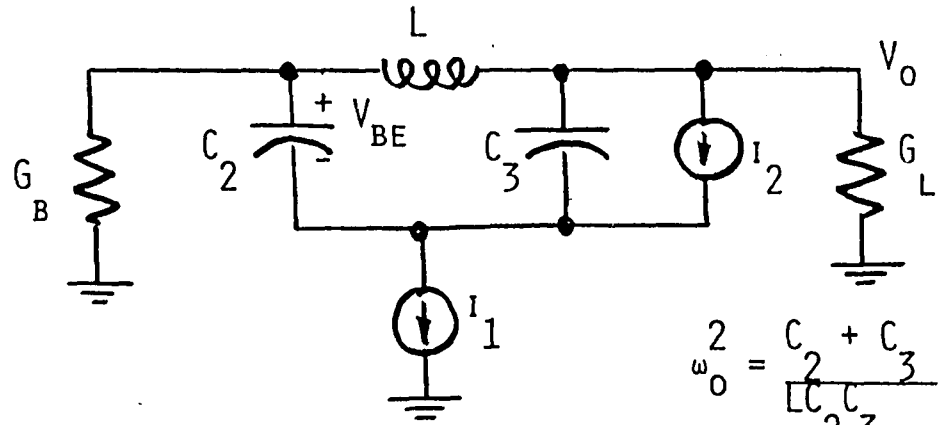

$I_1 = G_{M1} V_I$

$I_2 = G_{M2} V_{BE}$

$$\omega_O^2 = \frac{C_2 + C_3}{LC_2C_3}$$

Oscillator 'free-running' frequency

$G_{M2} = \frac{C_2}{C_3} G_L$ to compensate 'losses' in circuit

G_{M1} provides signal injection into Oscillator

$$\ddot{V}_O + \omega_O^2 V_O = \frac{G_{M1}}{C_3} \dot{V}_I$$

Phase Modulation in the Synchronous Oscillator

Linear Equation: $\ddot{V}_0 + \omega_0^2 V_0 = \frac{G_M}{C}\dot{V}_I$ (simplified notation)

Assume Solution: $V_0 = \bar{V}_0 \exp\left[j(\omega_I T + \theta_0)\right]$ $V_I = \bar{V}_I \exp\left[j(\omega_I T + \theta_I)\right]$

Define: $\phi = \theta_0(T) - \theta_I$ instantaneous differential phase

$\Delta\omega = \omega_0 - \omega_I$ instantaneous 'tracking' range

Transformed Equation: $\dot{\phi} = -3K\left(\sin\phi - \frac{\Delta\omega}{K}\right)$

where $K = \frac{G_M \bar{V}_I}{2C\bar{V}_0}$ Injection Constant for the Synchronous Oscillator

Condition for Synchronization: $\frac{\Delta\omega}{K} \leq 1$ (Lock-In)

Operational Modes: (1) Driven but Unlocked $\frac{\Delta\omega}{K} > 1$

(2) Driven and Locked $\frac{\Delta\omega}{K} \leq 1$

TRANSFER FUNCTION (GAIN-PHASE) FOR THE
SIMPLE SYNCHRONOUS OSCILLATOR CIRCUIT

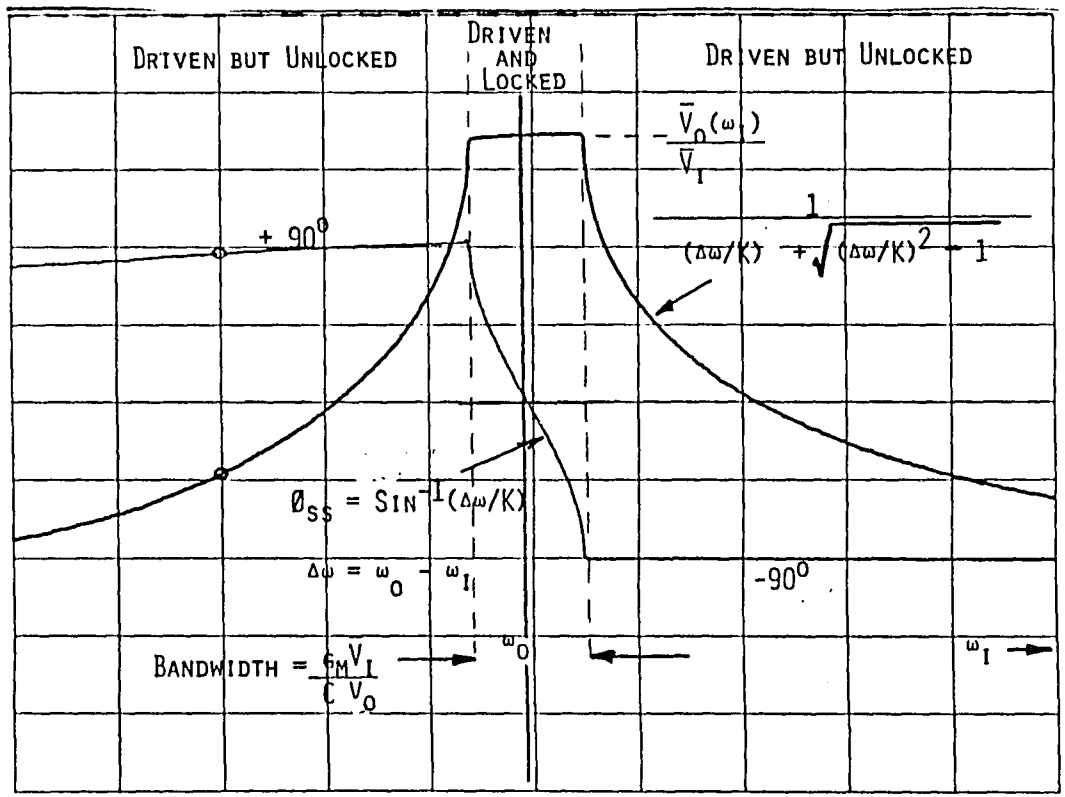

ADAPTIVE 'TRACKING' BANDWIDTH FOR THE SYNCHRONOUS OSCILLATOR

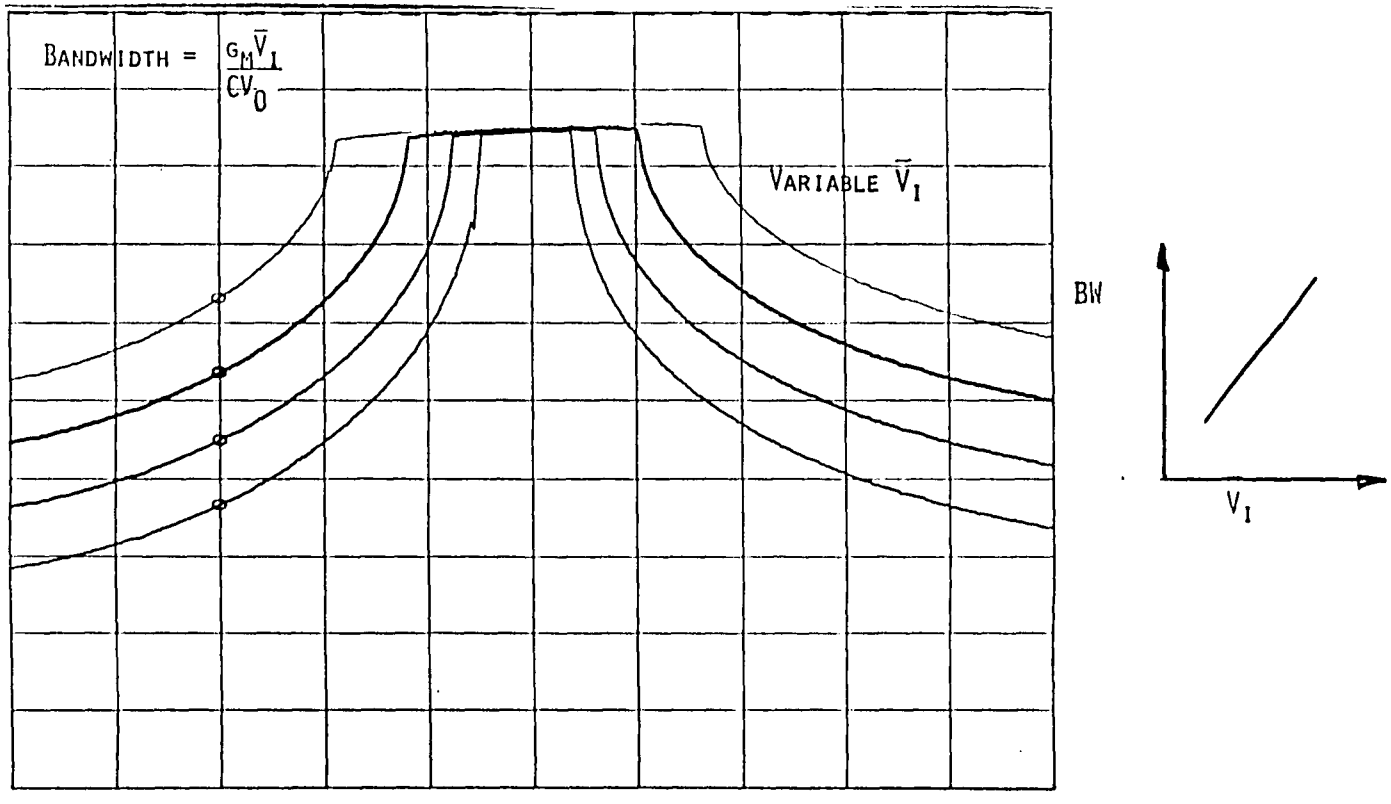

Phase Acquisition in the Synchronous Oscillator

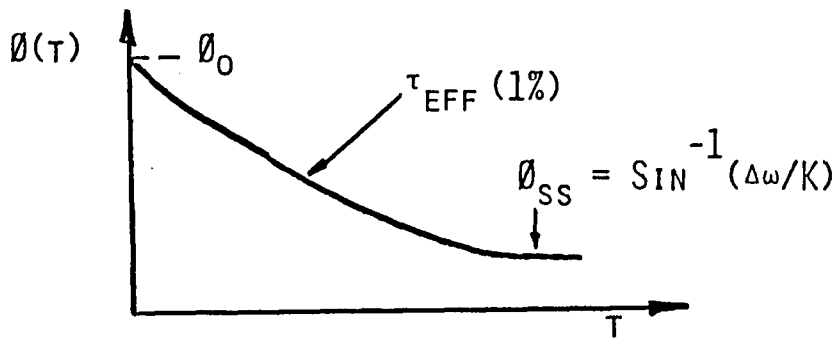

$$\tau_{EFF} = \frac{1}{K\sqrt{1 - (\Delta\omega/K)^2}}$$

$$\Delta\omega = \omega_0 - \omega_I$$

$$K = \frac{G_M V_I}{2C\ V_0}$$

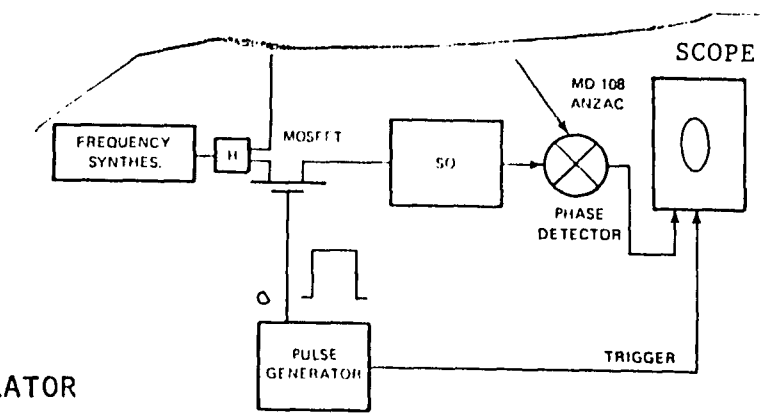

Test Set-up to Measure Acquisition and Storage in the Synchronous Oscillator

Harmonic 'Pumping' of the Synchronous Oscillator

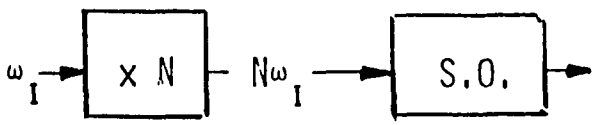

Analysis indicates:

(1) Increase in instantaneous 'tracking' bandwidth by factor of 'N' over simple S.O.

(2) Improved Selectivity (Filtering) by the ratio of $\frac{\omega_I}{\Delta\omega} \doteq Q$ of the S.O.

(3) For small deviations in Instantaneous 'tracking' bandwidth the phase acquisition is improved by a factor of 'N' over simple S.O.

(4) For small deviations in Instantaneous 'tracking' bandwidth the phase shift is reduced by a factor of 'N' over simple S.O.

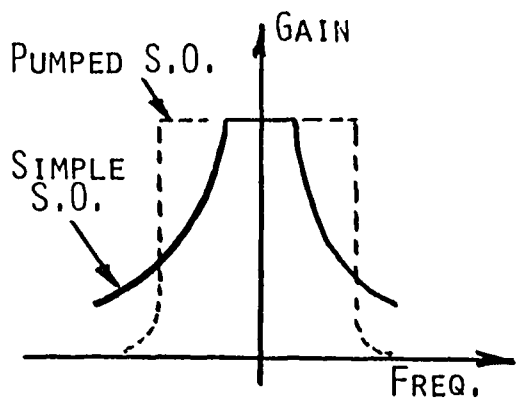

CONCLUSIONS

(1) THE SIMPLIFIED LINEAR ANALYSIS PROVIDES INSITE INTO THE OPERATION OF THE SYNCHRONOUS OSCILLATOR IN THE FOLLOWING AREAS:

- (A) CRITERIA FOR SYNCHRONIZATION (LOCKING)
- (B) ADAPTIVE 'TRACKING' BANDWIDTH
- (C) PHASE ACQUISITION
- (D) TRANSFER FUNCTION FOR SIMPLE AND HARMONICALLY PUMPED S.O.'S

(2) THE BASIC S.O. HAS SUPERIOR PERFORMANCE WHEN COMPARED WITH CONVENTIONAL APPROACHES (E.G. PLL'S) BECAUSE OF THE FOLLOWING FACTORS:

- (A) HIGH INTERNAL GAIN (NONLINEAR G_M)
- (B) UNIQUE SIGNAL INJECTION METHOD (TRANSCONDUCTANCE MULTIPLIER)
- (C) HIGH REGENERATION IN THE OSCILLATIONS (MULTIPLE FEEDBACK)
- (D) EFFICIENT HARMONIC PUMPING TECHNIQUE

(3) FUTURE RESEARCH SHOULD CONCENTRATE ON THE FOLLOWING AREAS:

- (A) ANALYSIS OF S.O. CONFIGURATIONS SUITABLE FOR INTEGRATION ON A CHIP
- (B) EXTENSION OF THE NONLINEAR METHOD TO UNDERSTAND S.O. OPERATION
- (C) CONTINUE EXPERIMENTAL CHARACTERIZATION AND MODELING

REFERENCES

[01] Runge, P.K.
Phase-Locked Loops with Signal Injection for Increased Pull-in Range and Reduced Output Phase Jitter.
IEEE Trans. Commun. COM-24:636-644, June, 1976.

[02] van der Pol, B.
Forced Oscillations in a Circuit with Non-linear Resistance.
Phil. Mag. S.7 3(13):65-80, January, 1927.

[03] Pengilley, C.J. and Milner, P.M.
On Asunchronous Quenching.
IEEE Trans. Automatic Control AC-12:224-225, April, 1967.

[04] Minorsky, N.
Comments on Asynchronous Quenching.
IEEE Trans. Automatic Control AC-12:225-227, April, 1967.

[05] Dewan, E.M.
Harmonic Entrainment of van der Pol Oscillations: Phaselocking and Asynchronous Quenching.
IEEE Trans. Automatic Control AC-17:655-663, October, 1972.

[06] Adler, R.
A Study of Locking Phenomena in Oscillators.
Proc. IRE 34:351-357, June, 1946.

[07] Kurokawa, K.
Some Basic Characteristics of Broadband Negative Resistance Oscillator Circuits.
BSJT :1937-1955, July, 1969.

[08] Uzunoglu, V.
Synchronization and tracking with Synchronous Oscillators.
In Proceedings of the 37th Annual Symposium on Frequency Control, pages 91-97. U.S Army ERADCOM and IEEE, 1-3 June, 1983.

[09] Uzunoglu, V.
Semiconductor Network Analysis and Design.
McGraw-Hill, 1964.

[10] Minorsky, N.
Non-linear Oscillations.
D. van Nostrand, 1962.

[11] van der Ziel, A.
Nonlinear Electronic Circuits.
John Wiley and Sons, 1977.

[12] Lindsey, W.C. and Simon, M.K.
Phase-Locked loops and their Applications.
IEEE Press, 1978.

VITA

Theodore D. Flamouropoulos was born in Thessaloniki Greece May 20, 1959 and immigrated to the United States at the age of twelve. He graduated with honors in June 1981 from Brown University with a Bachelor of Science degree in Electrical Engineering. He worked for one year with Dr. Jerry Daniels of Brown University at Kendrew Biosystems in San Diego California. Currently, he is a full time graduate student with the department of Computer Science and Electrical Engineering at Lehigh University.